

**U. S. A R M Y**  
**TRANSPORTATION RESEARCH COMMAND**  
**FORT EUSTIS, VIRGINIA**

AD 608522

TRECOM TECHNICAL REPORT 64-45

**THE DOMINANT AERODYNAMIC CHARACTERISTICS**  
**OF A SHAPED GEM**

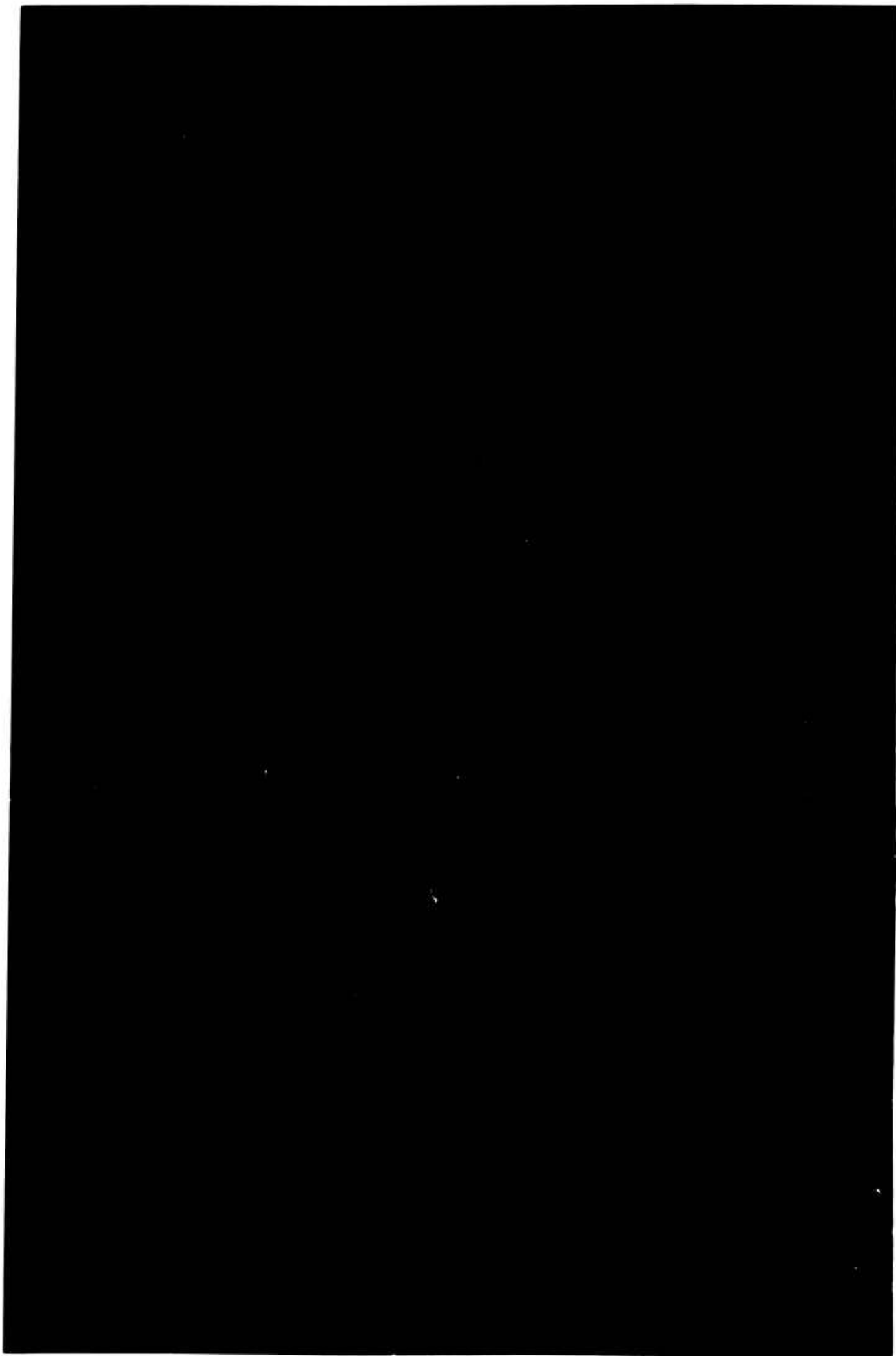
Task 1D021701A04803  
Contract DA 44-177-TC-850

September 1964

**prepared by:**

**PRINCETON UNIVERSITY**  
Princeton, New Jersey





#### DISCLAIMER NOTICE

When Government drawings, specifications, or other data are used for any purpose other than in connection with a definitely related Government procurement operation, the United States Government thereby incurs no responsibility nor any obligation whatsoever; and the fact that the Government may have formulated, furnished, or in any way supplied the said drawings, specifications, or other data is not to be regarded by implication or otherwise as in any manner licensing the holder or any other person or corporation, or conveying any rights or permission, to manufacture, use, or sell any patented invention that may in any way be related thereto.

★ ★ ★

#### DDC AVAILABILITY NOTICE

Qualified requesters may obtain copies of this report from

Defense Documentation Center

Cameron Station

Alexandria, Virginia 22314

★ ★ ★

This report has been released to the Office of Technical Services, U. S. Department of Commerce, Washington 25, D. C., for sale to the general public.

★ ★ ★

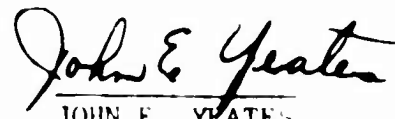
The findings and recommendations contained in this report are those of the contractor and do not necessarily reflect the views of the U. S. Army Mobility Command, the U. S. Army Materiel Command, or the Department of the Army.

HEADQUARTERS  
U S ARMY TRANSPORTATION RESEARCH COMMAND  
FORT EUSTIS VIRGINIA 23604

Interest in higher speed applications of air-cushion vehicles indicated a need for better understanding of the relationship between the lift, drag, and stability due to the air cushion and aerodynamic characteristics of the vehicle.

For the purpose of the investigation, the 20-foot-diameter P-GEM was modified for comparison with a 1/12 scale model. After correlation of the performance, a method was presented that permits prediction of full-scale performance in forward motion and the magnitude of control requirements for aerodynamically induced destabilizing forces.

  
WILLIAM E. SICKLES  
Project Engineer

  
JOHN E. YEATES  
Group Leader  
Aeromechanics Group

APPROVED.

FOR THE COMMANDER:

  
LARRY M. HEWIN  
Technical Director

**BLANK PAGE**

Task 1D021701A04803  
Contract DA 44-177-TC-850  
TRECOM Technical Report 64-45  
September 1964

THE DOMINANT AERODYNAMIC CHARACTERISTICS  
OF A SHAPED GEM

Report No. 684

Prepared by  
Princeton University  
Princeton, New Jersey

for  
U.S. ARMY TRANSPORTATION RESEARCH COMMAND  
FORT EUSTIS, VIRGINIA

by

A. F. Wojciechowicz, Jr.

W. B. Nixon

T. E. Sweeney

## FOREWORD

During the course of the experimental portion of this work it was found advisable to rework the control vanes in the P-GEM. These vanes, essentially butterfly valves, were originally pivoted about their 50% chord point and as such were unstable. New vanes pivoted at 25% chord not only improved control-feel and effectiveness but eliminated a control-system-induced instability of the craft.

The modified P-GEM showed a marked increase in static stability, the value of  $h/D$  for neutral stability in hover being increased from .05 to .08.

The replacement of the constantly fluttering unstable vanes with the new stable system also reduced lift horsepower required as can be seen in Figure 18 of this report. For this reason, previously run flight tests were repeated to enhance the validity of this report.

## TABLE OF CONTENTS

	Page
FOREWORD . . . . .	iii
SYMBOLS . . . . .	vii
SUMMARY . . . . .	1
INTRODUCTION . . . . .	2
GENERAL ANALYSIS . . . . .	4
WIND-TUNNEL TESTS . . . . .	16
FULL-SCALE FLIGHT TESTS . . . . .	19
CONCLUSIONS . . . . .	23
BIBLIOGRAPHY . . . . .	24
FIGURES. . . . .	25-43
DISTRIBUTION . . . . .	44

# LIST OF SYMBOLS

$P_B$	base pressure, gage, $\text{lb/ft}^2$
$P_{B_0}$	base pressure in hover, $\text{lb/ft}^2$
$P_{b_e}$	effective base pressure defined by $P_{b_e} S = \int_{\text{span}} P_L dS$ , $\text{lb/ft}^2$
$P_{b_0}$	theoretical base pressure $\text{lb/ft}^2$
$P_L$	gage pressure over lower surface, $\text{lb/ft}^2$
$P_u$	gage pressure over upper surface, $\text{lb/ft}^2$
$P_{T_j}$	jet total pressure, $\text{lb/ft}^2$
$P_j$	jet static pressure, $\text{lb/ft}^2$
$q_j$	jet dynamic pressure, $\text{lb/ft}^2$
$q$	free-stream dynamic pressure, $\text{lb/ft}^2$
$S_B$	base area bounded by the inside edge of the jet, $\text{ft}^2$
$A_j$	jet area, $\text{ft}^2$
$S_j$	jet area normal to the jet flow, $\text{ft}^2$
$S$	effective base area, $\text{ft}^2$
$L$	total lift, lb
$L'$	aerodynamic lift, lb
$D$	total drag, lb
$J$	jet momentum, $mv_j$ , lb
$C_L$	total lift coefficient, $L/qS$
$C_L'$	aerodynamic lift coefficient, $L'/qS$
$C_D$	total drag coefficient, $D/qS$
$C_{d_0}$	drag coefficient without blowing
$C_{\mu}$	jet momentum coefficient, $J/qS$

$c$	circumference of the jet centerline, ft
$h$	altitude, ft
$\theta_0$	initial jet angle measured from the vertical and negative inwards
$A$	augmentation ratio, $L/J$
$A'$	forward flight augmentation
$A_0$	augmentation in hover
$V_j$	jet velocity, ft/sec
$V_0$	forward flight velocity, ft/sec
$\dot{m}$	jet mass flow - slugs/sec
$\eta_A$	nondimensional coefficient defined by $P_{be} = A P_{b0}$
$\eta_L$	percentage of weight supported by the aerodynamic lift, $L'/w$
$\eta_{int}$	internal efficiency
$\eta_p$	propulsive efficiency
$h/D$	nondimensional height parameter
$w$	weight, lb
$mac$	mean aerodynamic chord

---

## SUMMARY

The effects of aerodynamic forces and moments acting on a ground effect machine in forward flight are investigated in some detail. Emphasis has been placed upon the performance gains possible by shaping a GEM to maximize lift at zero degrees angle of attack.

The associated longitudinal stability and trim problem is discussed, and at least one solution presented.

The work is both theoretical and experimental, the latter utilizing wind-tunnel models of a reconfigured P-GEM and also the full-scale P-GEM. Flight test results prove the validity of the concept and are extrapolated to higher airspeeds than those attainable with the P-GEM.

## INTRODUCTION

The several years of research looking into the fundamental characteristics of ground effect machines has convinced many people that substantial improvements in performance of these craft can be achieved by new concepts of the aerodynamic configuration of the machines.

Ground Effect Machines (GEM) research at Princeton University during recent years has been largely devoted to the examination of each extreme of a broad spectrum of configurations intended to yield favorable aerodynamic forces and moments of cruise velocities.

It was decided that at one end of such a spectrum of configurations, a useful GEM, because of mission requirements, might necessarily be "barge-like" in appearance. In order to take advantage of the relatively high dynamic pressures at which the craft might be expected to cruise, the addition of wings to the otherwise pure GEM has been most seriously considered. Investigations of this concept have been theoretical and experimental, the latter phase being both with wind-tunnel models and full-scale machines (Reference 1). Results of this work have proven that the hoped-for gains in performance and stability do, in fact, exist.

The other configuration extreme considered would be that shape determined from forward flight aerodynamic considerations alone. This might well be the case if the mission requirements did not seriously affect the configuration. Under such ground rules a designer, given free choice, would naturally attempt to arrive at a geometric shape which would optimize performance, static stability, and control. This report covers the progress made in these matters during the past year at Princeton University.

It is not suggested that the P-GEM (Figure 1) is an optimized GEM. It is, however, clear from four years' experience with the craft that its shape is responsible for many interesting forward flight characteristics. Chief among these is the effect of its aerodynamic cleanliness on performance and static stability. Principally because of this and also because the craft is still in excellent flight condition, its shape was selected as a basis for proving the predictions of an analytical study which constitutes the first portion of this work. Following this general analysis is a section reporting the results of selected wind-tunnel tests of a 1/12 scale model of the P-GEM and a final section of flight test results of the full-scale P-GEM.

The major hoped-for advantage of optimizing the aerodynamic shape of a GEM is an improvement in its cruise performance by generally improving the  $L/D$  of the craft. The P-GEM, for example, has a reasonably high cruise lift coefficient, as will be discussed in a subse-

---

quent section, which indicates that considerable gain in height may be achieved at even moderate cruising speeds. This may easily be seen by considering the craft as a wing. While it is not a very efficient wing, it is, considering the light base loadings, an effective wing at speeds of approximately fifty miles per hour. Since this craft has its center of gravity in its center, it may be considered a wing with a C.G. at  $.5 \text{ mac}$ ; and since it is basically a tailless craft, it is not surprising that strong longitudinal instability problems have arisen. Configuration changes designed to cope with this nose-up pitching moment are a major portion of this work.

## GENERAL ANALYSIS

The total lift of a GEM can be represented by the sum of its momentum thrust components and the lift produced by a pressure differential between the upper and lower surfaces. In hover, this pressure differential is the increase from ambient of the pressure under the base of the machine. If, however, the top surface of the GEM is shaped so that in forward flight increased velocities and, consequently, reduced pressures occur on the upper surface, the pressure differential between the upper and lower surfaces increases, providing additional lift of an aerodynamic nature. As will be shown in the following sections, this aerodynamic lift due to the topside pressure distribution can increase the performance of a GEM substantially. However, special care must be taken so that the distribution of this "topside" lift does not produce adverse stability and control characteristics.

In the following analysis, an attempt will be made to determine the nature of this "topside" lift and its effect upon GEM performance in the hope that it will bring a better understanding of the shaped GEM and establish some design criteria.

### LIFT

In general, any shaped GEM with annular jet blowing will produce a lift force equal to the pressure lift plus the jet reaction lift. The pressure lift can be written as

$$\text{pressure} = \int_{\text{span}} (P_L - P_U) dS \quad (1)$$

where  $P_L$  and  $P_U$  are the pressures over the lower and upper surfaces, respectively. The pressure over the lower surface of a GEM consists of the jet pressure acting on the jet area normal to the lift direction and the base pressure acting on the base area. In hover, the base pressure can be considered approximately constant while the jet pressure varies linearly across the jet area from a value equal to the base pressure at the inside edge to atmospheric pressure at the outside edge. Thus the average jet pressure can normally be approximated by one-half the base pressure. By using these assumptions, and further assuming that the jet and base pressures do not vary with forward flight, equation (1) can be rewritten as

$$\begin{aligned} L \text{ pressure} &= \frac{P_0}{2} A_j + P_0 S_0 - \int_{\text{span}} P_U dS \\ &= P_0 \left( S_0 + \frac{A_j}{2} \right) - \int_{\text{span}} P_U dS \end{aligned} \quad (2)$$

The second term of equation (2) represents the lift due to the pressure distribution over the top surface of the GEM.

At this point of its development, the pressure lift as given by equation (2) is somewhat incorrect because the action of the free stream in forward flight upon the jet curtain will have some effect on both the jet pressures and jet-induced base pressures. Although some work has been done experimentally, little effort appears to have been spent analytically determining just how these pressures vary with forward speed. An analytical approach is quite difficult and complex, particularly when a solution is sought for the general case. Thus, the difficulty of not being able to predict the change in pressure lift with velocity purely by analytical means leads to the nondimensional approach utilizing available experimental results given below.

If we define a base pressure,  $P_{Be}$ , such that  $P_{Be} = \int_{\text{span}} P_b dS$  at each velocity point, we can tentatively account for the change in base pressure with speed. By redefining the terms of equation 2 in this manner and summing this with the jet reaction lift, the total lift is found:

$$L = P_{Be} S_{Be} + J \cos \theta_o + L_{\text{aero}} \quad (3)$$

where  $L_{\text{aero}}$  is the aerodynamic lift due to the topside pressure distribution. Equation (3) is now put in coefficient form:

$$C_L = \frac{L}{qS} = \frac{P_{Be}}{q} + C_{\mu} \cos \theta_o + C_{L \text{ aero}}. \quad (4)$$

In hover, the effective base pressure can be fairly well approximated by the expression

$P_{Bo} = \int \frac{1 - \sin \theta_o}{h} \frac{c}{s}$  as predicted by simple momentum theory. Logically, if there is a decay in the effective base pressure with forward flight, this base pressure will be some fraction of the base pressure in hover. That is,

$$P_{Be} = \eta A P_{Bo} \approx \frac{\eta A \int (1 - \sin \theta_o)}{h} \frac{c}{s} \quad (5)$$

Also, it has been well established that the aerodynamic lift coefficient can be expressed as the lift coefficient without jet blowing plus a change in  $C_{L \text{ aero}}$  due to the increased circulation that results from blowing. From circulation control theory and empirical evidence, the change in  $C_{L \text{ aero}}$  due to blowing is a function of

$$C_{L \text{ aero}} = \frac{C_L}{C_{\mu=0}} + \Delta C_L(C_{\mu}) \quad (6)$$

Substituting equations 5 and 6 into equation 4 produces

$$C_L = \underbrace{\frac{\eta A S (1 - \sin \theta_o) C_{\mu}}{h} \frac{c}{s}}_{\text{Base Pressure Lift}} + \underbrace{C_{\mu} \cos \theta_o}_{\text{Reaction Lift}} + \underbrace{C_L' + C_L'(C_{\mu})}_{\text{Aerodynamic Lift}}. \quad (7)$$

Thus, for a given geometry, angle of attack, and altitude, the lift coefficient reduces to a function of  $C_{\mu}$  and  $\eta_A$ . Nothing has yet been said as to how  $\eta_A$  varies with speed; however, analysis of empirical evidence strongly indicates that  $\eta_A$  is a function of  $C_{\mu}$ . Qualitatively, it is readily seen that if  $\eta_A$  is dependent upon some forward flight parameter other than  $C_{\mu}$ , then the lift coefficient would be strongly dependent upon how  $C_{\mu}$  was derived. For example, if  $C_{\mu}$  was kept constant while changing jet mass flow, one would expect  $C_L$  to vary if  $\eta_A$  was not a function of  $C_{\mu}$ . Fortunately, wind-tunnel data shows that this is not the case. When plotted as a function of  $C_{\mu}$ , the lift coefficient falls on the same curve regardless of jet mass flow on free-stream dynamic pressure. A sample of the Grumman data presented in reference 2 is shown in Figure 2 to illustrate this. Thus, since  $\eta_A$  apparently is a function of  $C_{\mu}$ , the lift coefficient reduces solely to a function of  $C_{\mu}$ , and this function completely defines the lift coefficient for geometrically similar GEMs, if Reynolds number effects are overlooked. On the strength of this argument, it will be assumed throughout this analysis that model lift data presented as a function of  $C_{\mu}$  correlates directly to an estimate of full-scale performance.

At this time the author would like to point out that due to the lack of published data in the field of shaped GEMs, references 2 and 3 will be relied on heavily for experimental support of this paper. The model used in references 2 and 3 was a three-dimensional, half-span, reflection plane airfoil with an 18-percent thick modified Clark Y profile. An external air supply piped through the tunnel floor fed the peripheral jet. It is to be noted that feeding the jet in this way neglects the presence of an air intake on the topside surface which is inherent to the design of nonrecirculating type GEMs. This means that the streamline flow over the top surface was somewhat unrealistic, and the effect on the base pressure of increased pressures at the air intake with forward velocity was not realized. However, in spite of this, the data can be used to demonstrate the experimental method for determining the forward flight characteristics of shaped GEMs, and the effect of the aerodynamic lift upon its performance.

#### EFFECT OF THE AERODYNAMIC LIFT TERM UPON PERFORMANCE

##### Altitude

Thus far in this analysis, it has been assumed that there is a decay in the base pressure lift with speed because there are strong indications that this occurs on models which are externally fed (see references 2, 3, and 4). However, this fact has not been substantiated for GEMs which have an intake on the topside surface. It can reasonably be surmised that with forward speed there will be a pressure recovery at the inlet which will raise the jet and base pressures as forward speed builds up. Consequently, if this effect of the inlet

is superimposed upon the base pressure decay found for externally fed GEMs, the expected magnitude of the decay is considerably diminished. In fact, for some GEM designs the decay may even be negligible. In any case, if it is assumed that the aerodynamic lift builds up much faster than the base pressure decay, then the vehicle must rise in altitude because, with forward speed, the lift required of the cushion to support the weight of the vehicle is reduced. In the analysis which follows, a simplified approach will be taken to vividly show this effect of aerodynamic lift upon altitude.

In hover the lift equation for a GEM in terms of its augmentation ( $A_0$ ), weight ( $W$ ), and jet momentum ( $J$ ) is given by

$$W = A_0 J \quad (8)$$

If in forward flight the jet momentum is held constant and aerodynamic lift of magnitude  $L$  is produced, the lift equation becomes

$$W - L = A' J \quad (9)$$

where  $A'$  is the forward flight augmentation required from the base. Substituting  $A_0 = \frac{W}{J}$  into equation (9) produces

$$A_0 \left(1 - \frac{L}{W}\right) = A' \quad (10)$$

Equation (10) expresses the fact that the base augmentation required to support the weight of the machine decreases as the aerodynamic lift unloads the base of the vehicle. To approximate how this decrease in the base augmentation required of the base affects the altitude, Chaplin's simple momentum theory for the augmentation is used while once again assuming that the decay in the pressure term can be represented as some fraction ( $\eta A$ ) of that in hover.

$$A' = \cos \theta_0 + \frac{\eta A (1 - \sin \theta_0)}{h \cdot c/s} \quad (11)$$

Solving equation (11) for the nondimensional altitude  $h \cdot c/s$  yields

$$h \cdot \frac{c}{s} = \frac{\eta A (1 - \sin \theta_0)}{A' - \cos \theta_0}$$

or

$$h \cdot \frac{c}{s} = \frac{\eta A (1 - \sin \theta_0)}{A_0 \left[1 - \frac{L}{W}\right] - \cos \theta_0} \quad (12)$$

From equation (12) it is seen that if the decrease in  $\eta A$  is small compared to the build-up of aerodynamic lift with speed, then the altitude must increase if the jet momentum is held constant. To determine the effectiveness of the aerodynamic lift for increasing altitude, equation (12) is differentiated with respect to the percentage of the weight supported by the wings ( $\frac{L}{W}$ ).

Denoting  $\frac{L}{W}$  as  $\eta_L$

$$\frac{d(\frac{h}{r_0})}{d \eta_L} = \frac{1}{A_0} \frac{(1 - \sin \theta_0) \eta_A}{\{A_0(1 - \eta_L) - \cos \theta_0\}^2} \quad (13)$$

Examination of equation (13) brings out an important aspect of the shaped GEM concept. Since the hover augmentation appears in the denominator of expression (13), it can be concluded that the greatest altitude increase due to aerodynamic lift will occur with vehicles that operate at the least hover augmentation. Furthermore, the aerodynamic lift more effectively increases altitude as greater lift is produced. In essence the first statement means that shaping a GEM to produce aerodynamic lift is most suitably applied to vehicles of the lighter base loadings because they usually operate with lower augmentation than do vehicles of higher base loadings. This result is clearly seen graphically in Figure 3. In Figure 3 the theoretical augmentation curve for a circular GEM is plotted against the non-dimensional altitude  $h/r_0$ , where  $r_0$  is the radius of the machine. By noting the slope of the augmentation curve, it is seen that at the higher augmentations, an appreciable decrease in the base augmentation is necessary before a significant increase in altitude is realized. On the other hand, at the lower augmentations, a decrease in the base augmentation brings about a relatively greater altitude increase. Thus, the altitude gain due to aerodynamic lift depends upon at which part of the augmentation curve the GEM operates in hover.

To illustrate the magnitude of the altitude increase which shaped GEMs could quite feasibly be capable of, the data of reference 2 was used to obtain the curves shown in Figure 4. In these plots the lift coefficient was multiplied by  $1/C_M$  and plotted against  $1/C_M$  for several altitudes. The value of plotting the data in this way is that:

1. It yields a finite hover point equal to the hover augmentation ( $L/W$ ) at  $1/C_M = 0$ .
2. The velocity increases as  $1/C_M$  increases.
3. If the jet momentum is held constant, the value of  $\frac{C_L}{C_M} = \frac{W}{J}$  remains constant for a particular vehicle throughout its speed range.

Thus, for constant jet momentum, a plot of  $C_L/C_M$  vs.  $1/C_M$  is a horizontal line extending from the hover point.

For example, suppose a vehicle geometrically similar to the model used in reference 2 was designed to operate in hover at a scale height corresponding to 2.5 inches for the model. Referring to Figure 4, we see that this corresponds to a lift augmentation of 3.4 in hover, or  $C_L/C_M = 3.4$  throughout its speed range, if the jet momentum is held constant. Thus we see that the altitude triples at  $1/C_M$  equal to 3.1.

### Power Required

The power required for a GEM in forward flight consists of two parts, the power required for lift and the power required for propulsion. The jet power required for lift in terms of the total jet pressure is given by

$$P_c = V_j S_j P_{Tj} = V_j S_j (P_j + q_j) \quad (14)$$

where  $P_j$  and  $q_j$  are the static and dynamic pressures of the jet, respectively. Analytically, the jet dynamic pressure can easily be related to the jet momentum if a constant velocity jet is assumed. However, difficulty arises when one tries to relate the jet static pressure to any one parameter. Qualitatively, it can be seen that the base loading, i.e., back pressure in the jet, will have a large bearing on the static pressure. Also, the action of the free-stream pressures on both the inlet and upon the jet itself will have some effect upon the jet static pressures. Accounting for all these effects in developing the static pressure term would be very nice indeed; however, the complexity of the problem does not lead to a clearly understood solution. Thus, as a matter of expediency, some assumptions must be made. The first of these assumptions is that the free-stream effects on the inlet and the jet curtain cancel each other so that there is no base pressure decay with forward flight. Secondly, it has been shown that in hover and in slow forward flight, the mean jet static pressure is approximately one-half the base pressure. It will be assumed that this holds true throughout the entire speed regime.

Using the above assumptions, the jet power required for a GEM with no aerodynamic lift is given by

$$P_c = \frac{1}{2} \rho S_j V_j^3 + S_j V_j \frac{W \cos \theta_0}{2 S_b} \quad (15)$$

where  $S_j$  is the jet nozzle area normal to the flow and  $S_b$  is the area of the base including one-half the nozzle area. Since  $\dot{V} = A$  and  $\dot{V} = \rho S_j V_j^2$  for a constant-velocity jet, equation (15) can be rewritten as

$$\text{Power (cushion)} = \frac{1}{2} V_j W \left\{ \frac{1}{A} \left( 1 - \frac{S_j}{S_b} \cos \theta_0 \right) + \frac{S_j}{S_b} \right\} \quad (16)$$

The power required for propulsion is simply the total drag multiplied by the velocity. By assuming zero momentum recovery, the total drag can be written as

$$D = C_D q S_b + m_j V_0$$

where  $C_D$  is the aerodynamic drag coefficient. Thus the propulsive

power can be written as

$$\text{Power} = \frac{V_o (C_D q S_b + \dot{m} V_o)}{\text{Propulsion}} \quad (17)$$

By combining equations (16) and (17), the total brake horsepower required is obtained:

$$\text{BHP}_r = \frac{1}{1100} \frac{V_j W}{\eta_{INT}} \left\{ \frac{1}{A} \left( 1 - \frac{S_j}{S_b} \cos \theta_o \right) + \frac{S_j}{S_b} \right\} + \frac{V_o}{550} \frac{(C_D q S_b + \dot{m} V_o)}{\eta_P} \quad (18)$$

As developed previously for a shaped GEM, the weight supported by the cushion equals  $W(1 - \eta_L)$  and the forward flight augmentation equals  $A_o(1 - \eta_L)$ . Substituting these values into equation (18) yields the power required for the shaped GEM,

$$\text{BHP} = \frac{W(1 - \eta_L)}{1100 \eta_{INT}} \left\{ \frac{(1 - \frac{S_j}{S_b} \cos \theta_o)}{A_o(1 - \eta_L)} + \frac{S_j}{S_b} \right\} + \frac{V_o}{550 \eta_P} (C_D^* q S_b + \dot{m} V_o) \quad (19)$$

where  $C_D^*$  represents the drag coefficient including induced aerodynamic drag.

If we examine equation (19) from the viewpoint of keeping the jet momentum constant, allowing the vehicle to rise as aerodynamic lift builds up, it is seen that the first term represents a decrease in the horsepower required from that of a nonshaped GEM. The reason for this is that as aerodynamic lift unloads the base, the static pressure requirement of the jet is reduced. Although the magnitude of this decrease as shown in equation (19) may be questionable due to the assumptions made for the static pressure, it appears that this decrease in power required can compensate for a good part or all of the power required due to the induced aerodynamic drag. Thus, there is a good possibility that even though aerodynamic lift increases the altitude capability of a shaped GEM, it may have only a small effect on the total power required.

A second large effect of aerodynamic lift is seen when the altitude is held constant while the jet momentum is reduced as aerodynamic lift builds up with velocity. In this case both the jet velocity and mass flow decrease with forward speed. Therefore, the power required for both lift and propulsion is reduced from that of a comparable nonshaped GEM. The important significance of this is that, if so desired, a shaped GEM should be capable of cruising at the same altitudes with less power and more economy than a comparable nonshaped GEM.

## DRAG

Since a shaped GEM produces lift in forward flight, its drag components form an interesting combination of those found for both an airplane and a ground effect machine. Classically, the drag of an airplane consists of its parasite and lift-induced drag. Similarly, the drag of a shaped GEM consists of an induced drag term plus those terms normally found for a GEM.

$$D = D_{\text{parasite}} + D_{\text{induced}} + D_{\text{momentum}}$$

or

$$D = C_D q S = (C_{Dp} + C_{Di} + C_{Dm}) q S \quad (20)$$

The parasite drag term in equation (20) represents skin friction drag and the form drag which includes pressure drag due to the shape of the vehicle exposed to the free stream and curtain drag. Normally this drag is determined experimentally by attaching a simulated jet curtain to a model and determining the drag coefficient at zero lift. The momentum drag is a term peculiar to "air eating" devices such as GEMs, and results when a stream tube of air is turned 90° into the intake of the vehicle and is brought to zero velocity in the settling chamber. The drag force equals the total loss of horizontal momentum of the mass of air entering the intake, and is therefore equal to . . . . However, full-scale and model studies have shown that the total drag as given by equation 20 predicts a higher than actual drag when a full momentum loss is considered. To account for this, it has been argued that since flow is exhausted through annular jets, part of the jet flow eventually turns in the downstream direction before it expands out to ambient, causing a momentum "recovery" in the form of a thrust. From a physical standpoint, it seems improbable that a direct thrust force is transmitted back through the jet to the vehicle itself unless the jet angle is such that a direct jet reaction component is in the thrust direction. However, there is a good possibility that the front and rear jets induce pressures in the vicinity of the leading and trailing edges in such a way that a jet-induced pressure thrust is developed in a manner analogous to that of a jet-flapped wing. If this is the case, the cause of the apparent drag reduction mentioned above would seem to be more closely related to a reduction in form drag due to blowing rather than a direct result of "momentum recovery", as such. Actually it makes no large difference how this phenomenon is accounted for. Some people may prefer to add a correction factor to the momentum drag term, while others may prefer to assume a full momentum loss and account for the drag reduction in the parasite drag term. However, the author would like to let the above example suggest that from an academic standpoint, labeling the cause of the drag reduction as "momentum recovery" may be a misnomer. There is no real proof that "momentum recovery" actually exists, and as

pointed out above, the drag reduction could quite feasibly arise from some other effect of jet blowing, which in turn may be a function of the jet momentum.

The induced drag or trailing vortex drag term in equation 20 represents the kinetic energy lost by the system in the generation of trailing tip vortices. In finite wing theory this is interpreted as the component of lift in the drag direction that results from downwash. Normally, the pressures over the topside surface of a GEM are close to ambient; so if any tip vortices are generated in forward flight, their strength is small, and the resultant drag can usually be neglected. However, the reduced pressures over the upper surface of a shaped GEM cause the formation of tip vortices of comparatively higher strength. Flow visualization of circular models has shown that the forward part of the annular jet rolls up into a horseshoe type vortex system that translates around the front perimeter of the model, blending with and strengthening the familiar trailing vortices at the wing tips. This strengthening of the trailing vortex system by the jet flow in the area of the wing tips represents a loss in jet energy which is felt by the vehicle in the form of induced drag. Also, due to the close association of the trailing vortex strength and total circulation, this can most likely be interpreted as the induced drag caused by the increased circulation due to blowing.

For a shaped GEM, the total circulation about the airfoil is the circulation without blowing plus the increase in circulation due to blowing. Since the total circulation determines the aerodynamic lift, it can be shown in a manner analogous to that used in finite wing theory that the induced drag coefficient can be expressed as

$$C_{Di} = \frac{C_L'^2}{\pi A e} \quad (21)$$

where  $C_L'$  is the aerodynamic lift coefficient and  $A$  is the aspect ratio. The efficiency factor  $e$  is a term which must be determined experimentally and most likely will vary with the wing lift distribution, jet momentum coefficient, and altitude.

By substituting the expressions for the drag components developed above into equation (20), the total drag coefficient can be written as

$$C_d = C_{dp} + \frac{C_L'^2}{\pi A e} + \frac{\dot{m} V_o}{q S_b} \quad (22)$$

It is to be noted that for reasons stated above, the author has chosen the alternative method of accounting for the apparent drag reduction in the parasite drag term while assuming a full momentum loss. As in the case for the lift coefficient, all the terms of equation (22) will vary with forward speed. Thus, if model test data is to be applicable for full-scale considerations, some forward flight correlation para-

meter must be found. Toward this end, the results of recent model tests with externally fed GEMs have been very enlightening. In reference 3 it was found that although drag data did not seem to correlate well with  $C_{\mu}$ , the data did correlate when plotted as a function of the ratio of the free-stream dynamic pressure to the critical dynamic pressure at which the front curtain passes under the base. Analytically, the expression used for calculating  $q/q_c$  was  $q/q_c = \left( \frac{\rho V_o h a}{2 \dot{m}} \right)^2$ . Al-

though there is no doubt that the discovery of this correlating parameter is an important step towards an understanding of how the drag coefficient varies with speed, it should be pointed out that  $q/q_c$  as defined in the above equation is actually a function of  $1/C_{\mu}$ . This may be shown as follows:

$$C_{\mu} = \frac{\dot{m} V_j}{q S} = \frac{q_j S_j}{q S} \quad , \quad \therefore \quad q/q_j = \frac{S_j}{2 C_{\mu} S_b}$$

$$q/q_c = \left( \frac{\rho V_o h a}{2 \dot{m}} \right)^2 = \frac{V_o^2 (h a)^2}{4 S_j^2 V_j^2} \quad , \quad \therefore \quad \frac{V_o^2}{V_j^2} = \frac{q}{q_j} = \frac{4 S_j^2 q}{(h a)^2 q_c}$$

$$\therefore \quad \frac{S_j}{2 C_{\mu} S_b} = \frac{4 S_j^2 q}{(h a)^2 q_c} \quad \text{OR} \quad \frac{q}{q_c} = \frac{(h a)^2}{8 S_j S_b C_{\mu}}$$

For this reason, the Grumman lift data presented in references 2 and 3 correlated equally well with both  $C_{\mu}$  and  $q/q_c$ . The drag data of reference 3 did not, however, correlate also with  $C_{\mu}$ . One possible explanation is that  $C_{\mu}$  is a difficult parameter to ascertain accurately because a measurement of the jet velocity distribution must be made, whereas for an externally fed GEM the jet mass flow, and consequently  $C_{\mu}$ , can be determined quite accurately. At the same time, the measured drag forces are of a smaller magnitude and subject to greater tare corrections than are the lift forces. For this reason, errors in determining  $C_{\mu}$  could show up as a far greater scatter of the data for drag than it would for lift. This explanation is offered here for consideration by others.

In any case, the important fact is that there appears to be a correlating parameter for the drag of externally fed GEMs. To illustrate this, a sample of the data presented in reference 3 is plotted in Figure 5. As seen in Figure 5, the reduction in the parasite drag coefficient due to blowing is quite noticeable at the lower  $q/q_c$  values. In fact, at the lower  $q/q_c$  values the net effect of blowing is a thrust which tapers off to a drag force at the higher  $q/q_c$  values.

Since the drag of an externally fed GEM does not include momentum drag,

the change in the momentum drag coefficient with velocity has to be considered to completely describe the dependence of the total drag coefficient upon velocity. It can easily be shown that if a constant velocity jet is assumed,  $C_{D_m}$  will be the same for all geometrically similar GEMs at a given value of the jet momentum coefficient. Thus in the light of what has been said above, the variation of all the drag coefficient terms of equation 22 with speed may be completely described by the common parameter  $C_\mu$ . If this is the case, then the total drag coefficient would be a function of  $C_\mu$ , and this function would completely describe the drag coefficient for all geometrically similar GEMs, if Reynolds number effects are neglected. However, if it is verified through further experimental studies that the variation of the parasite and induced drag terms are actually functions of  $q/q_c$  and not  $C_\mu$ , the problem still can be easily handled. In this case the full momentum drag would have to be subtracted out of drag measurements, and the remaining sum of the parasite and induced drag coefficients could be determined as a function of  $q/q_c$ . Since the drag reduction due to blowing would be included in the parasite drag term, the momentum drag computed on the basis of zero recovery could be added when making drag calculations.

#### PITCHING MOMENT

Shaped circular GEMs, such as the P-GEM, are usually loaded so that the center of gravity is at the 50% chord point so as to be balanced in hover. Unfortunately, due to its symmetric shape the resultant aerodynamic lift acts well forward of the C.G. Thus, an increasing nose-up moment develops as aerodynamic lift builds up with speed. Even without aerodynamic lift, it appears that a good many of the operational GEMs to date have a high-velocity stability requiring fairly large control forces to trim the nose-up moment as speed increases. Therefore, in this particular case of the shaped GEM, additional demands are made of the control system for trimming the aerodynamic nose-up moment. Unless very large control forces are available, the vehicle will run out of control at some speed and will pitchup. A nose-up at this point creates greater aerodynamic lift forward of the C.G., causing an increasing unstable attitude in pitch. Fortunately, when this maneuver was inadvertently carried out on the P-GEM, the speed dropped rapidly enough that the vehicle settled smoothly to the ground before any serious damage was done.

To avoid this limitation on speed, any aerodynamic surface such as a tail or swept wing could be placed so as to move the flying aerodynamic center aft to coincide with the C.G. Towards this end any non-blowing surface located aft of the C.G. would help, but a high tail or a swept wing seems to be the most likely prospect because a high tail would be a convenient solution and swept wings would most likely increase the effective aspect ratio.

There is not very much that can be said about this adverse effect of aerodynamic lift upon pitching moment except that the problem is recognized and something must be done about it if the beneficial effects of aerodynamic lift are to be utilized. Shaping the GEM with nonblowing surfaces as suggested above is one approach to a solution, and the results of recent model studies applying this approach is forthcoming in a separate report. Another approach may be a study of the effects of the intake position upon the pitching moment. It is a well known fact that the position of a suction slot on the top surface of an airfoil radically changes the pressure distribution over the topside surface in such a way that the pitching moment and longitudinal stability is altered considerably with no adverse effects upon the aerodynamic lift. Possibly, then, there is a favorable position for the intake which may alleviate the nose-up problem.

## WIND-TUNNEL TESTS

### CONFIGURATIONS TESTED

In order to cope with the severe pitch-up characteristics of the P-GEM due to its circulation lift, several configuration modifications were desired. These are:

1. Beaver tail modification
2. Swept delta wing modification
3. Geared trimmer configuration

The first two of these configurations, the beaver tail and the swept delta wing, are shown in Figures 6 and 7. They have in common the lengthening of the mac of the planform in the aft direction. Thus, with the C.G. position unaltered from the original circular configuration, the C.G. is effectively moved forward relative to the mac. In each of these modifications the original circular peripheral nozzle was maintained, and the addition was not fitted with nozzles of any kind.

The third configuration tested in the wind tunnel is shown in Figure 8. It is the result of designing, by aircraft considerations alone, the horizontal tail required for trimmed flight through a modest range of angle of attack. Such a stabilizer is of necessity extremely large relative to the plan area of the GEM. This is due to the C.G. being located at 50% of the mac and due to the quite short tail moment arm. To avoid the large-size fixed stabilizer which would be needed to cope with the pitching moments generated by the P-GEM configuration, a geared trimmer was designed. This trimmer as shown in Figure 8 is one-fifth the area required for a fixed stabilizer. In concept it is servo-actuated and geared 5 to 1 to the P-GEM; thus, a one-degree change in attitude of the craft produces a five-degree change in angle of attack of the trimmer. Such a scheme is limited by the stalling angle of the trimmer (in this case  $\pm 15^\circ$ ); this, however, permits an angle of attack change of  $\pm 3^\circ$  for the craft, which was deemed adequate for the cruising regime of a high-speed GEM.

The basic model (see Figure 9), a 1/12 scale model of the P-GEM, was altered to each of these configurations and tested in the Princeton 2 foot x 3 foot subsonic wind tunnel fitted with a ground plane. Tests were conducted to determine the effect of angle of attack, momentum coefficient ( $C_M$ ), and height above the ground plane on lift, drag, and pitching moment for each configuration. Momentum coefficients examined were  $C_M = 0$  and  $C_M = .04$ , and the ground clearances tested were  $h/D = .09$ ,  $.19$ , and  $\infty$ . The model was self-powered, which limited the upper value of  $C_M$ ; however, the self-powered model had the advantage of simulating the actual flow conditions into the scaled inlet

and the added advantage of including the correct momentum drag in the results.

## TEST RESULTS

### Beaver Tail Configuration

Figure 10 shows the basic characteristics of the beaver tail configuration at  $C_{\mu} = 0$  for three values of  $h/D$ . It will be noted that the ground proximity does not change the angle of zero lift but does have a pronounced effect upon the slope of the lift curve showing a substantial increase of  $dC_L/d\alpha$  with decreasing values of  $h/D$ . Drag changes due to the presence of the ground plane also appear to be typically affected, that is, a reduction of  $C_D$  with decreasing values of  $h/D$ . Most important, however, for the purposes of this study is the effect of the modification upon static stability. It will be noted that at  $C_{\mu} = 0$  the pitching moment curve indicates an unstable craft that is little affected by the value of  $h/D$  except for a small trim change with height change.

Figure 11 presents the characteristics of the same configuration under identical test conditions except that in this case  $C_{\mu} = .04$ . Of most significance is the dramatic increase of lift coefficient at  $\alpha = 0$  with a decrease in height, the much higher induced and momentum drag, and the alteration of the pitching moment curves with increasing  $h/D$  at a  $C_{\mu} = .04$ . It appears from these results that the craft would be at least neutrally stable at  $h/D = .09$  at the higher values of lift coefficient; however, increasing values of  $h/D$  appear to be destabilizing.

### Swept Delta Wing Configuration

The lift, drag and pitching moment characteristics of the swept-delta-wing P-GEM configuration are shown in Figures 12 and 13. For the  $C_{\mu} = 0$  case the most noteworthy result is the neutral longitudinal stability that was achieved at all values of  $h/D$ . When the momentum coefficient was increased to  $C_{\mu} = .04$ , however, some deterioration in this stability occurred, principally at the lower values of  $h/D$ . Also of considerable significance is the quite high lift coefficient attained at zero angle of attack ( $C_L = 0.6$  for  $C_{\mu} = .04$ ).

$\alpha = 0^\circ$

### Geared Trimmer Configuration

The third modification of the basic P-GEM shape to be tested was the geared trimmer device.

The results of these tests are presented in Figures 14, 15 and 16. Figure 14 shows that for  $C_{\mu} = 0$  the configuration is still statically

unstable but that the magnitude of the instability is essentially invariant with  $h/D$ . This trend is approximately unchanged for the case of  $C_{\mu} = .04$  (Figure 15). It will be noted in this figure that the lift coefficient for zero angle of attack compares favorably with similar characteristics of the swept delta wing configuration under the same conditions of angle of attack,  $h/D$  and  $C_{\mu}$ .

In order to determine the range of angle of attack that the geared trimmer would trim the P-GEM in forward flight, additional tests were run in the wind tunnel with the trimmer set at  $-10^{\circ}$ ,  $0^{\circ}$  and  $+10^{\circ}$  angles of incidence. The results of this work are presented in Figure 16, which shows the variation of the lift curve displacement with trimmer angle of incidence and clearly shows that for the range of trimmer angles tested the P-GEM could be trimmed through a range of lift coefficients from  $C_L = .5$  to  $C_L = .1.0$ .

## FULL-SCALE FLIGHT TESTS

### GENERAL DESCRIPTION OF CONFIGURATION

The over-all intent of the experimental portion of this work was to prove that a GEM can be so configured as to produce useful cruise lift coefficients in the sense that power, speed, ground clearance, and gross weight trade-offs could be made as a result of aerodynamic lift. In order to utilize these advantages, however, the craft must be adequately stable and trimmable throughout a useful range of lift coefficients. It was the specific intent of the wind-tunnel study, reported upon in the preceding section, to provide information for an optimum configuration of the P-GEM which would permit full-scale measurements of these important parameters.

A careful review of the effect of  $h/D$ ,  $C_{\mu}$ , and angle of attack upon the lift, drag, and pitching moment of the three configurations considered resulted in the selection of the geared trimmer for the following reasons:

1. The high cruise lift coefficients obtainable ( $C_L = .6 @ \alpha = 0^\circ$ ).
2. The wide range of lift coefficients through which the craft could be trimmed ( $C_L = .25 \rightarrow C_L = 1.25$  for  $i_t = \pm 15^\circ$ ).
3. The ease of obtaining artificial longitudinal stability, if desired, by servo-operating the trimmer.
4. The relative ease of physically accomplishing the modification of the P-GEM.

Although the original concept of the trimmer was to provide artificial longitudinal stability by means of a sensor and servo system, it was deduced that the response of the P-GEM to a disturbance would be such that the servo system would not be needed. Accordingly, the trimmer, when installed, was connected directly to the pilot's control stick, which operates in the usual airplane sense. This method of controlling the trimmer angle of incidence was found to be completely satisfactory, and all flights since its installation have used this system. A general view of the P-GEM fitted with the horizontal tail trimmer is shown in Figure 1.

### FLIGHT TEST INSTRUMENTATION

In order to measure the effect of aerodynamic lift upon the performance of the P-GEM, it was necessary to design and develop a height sensor which would combine high sensitivity, good damping, and adequate reliability. It was necessary that the performance of the height sensor would be unaffected by moisture, temperature changes, and forward movement of the craft. All of these requirements were met by a simple articulated four-leg device fitted with a linear potentiometer, the output of which was presented to the pilot on a millivoltmeter located

in the cockpit. A photograph of the P-GEM with the height sensor extended is shown in Figure 17. The only other required instrumentation was that normally provided in the P-GEM.

## TESTS

Repeated tests were conducted along a paved airstrip measuring the change in height of the craft with both airspeed and lift power setting. The technique employed was first to carefully measure hover height for a fixed lift power setting at one end of the runway. This was followed by an application of a given percentage of thrust power, which then remained constant throughout the run. The maximum height during the run was recorded by the pilot, and the stabilized ground speed was measured by a pacing automobile with a calibrated speedometer. Four repeat runs were made for each thrust power and lift power combination. It is interesting to note that the simplicity of these techniques and of the instrumentation resulted in a trouble-free test program with a high degree of repeatability in the data.

## TEST RESULTS

By means of sea-level power curves for the Lycoming VO-360 engine, with which the P-GEM is equipped, brake horsepower was determined for each of several hover heights. These results are shown plotted in Figure 18. It will be noted that this figure shows two BHP vs. height curves, the one labeled 1964 being substantially superior to that for 1963. This reflects a marked improvement in internal efficiency of the P-GEM brought about by reworking the control vanes situated in the peripheral nozzle (reference 5).

Figure 19 shows a direct plot of flight test results showing the variation in ground clearance with forward speed for several values of lift brake horsepower. It will be noted that a height decay occurs prior to speeds at which aerodynamic lift begins to become significant. This loss in ground clearance is minimal and seems to be most pronounced at a forward speed of approximately 20 miles per hour. This loss is, however, rapidly made up at slightly higher speeds and it is evident that at speeds of 30 to 35 miles per hour ground clearance is approximately 10% greater than the initial hover values.

The lift augmentation curves shown in Figure 20 were constructed from values of ground clearance and brake horsepower taken from Figure 19 for both the hover condition and for an airspeed of 35 miles per hour and are based upon an  $m_j v_j = 1.5$  pounds per brake horsepower at the nozzle. The extrapolation of the hover lift augmentation curve was accomplished by reference to previous P-GEM flight test results (reference 5). In order to predict, with reasonable accuracy, the performance of the P-GEM at speeds in excess of 35 miles per hour, it was necessary first to determine the level flight lift coefficients

as a function of  $h/D$ . Referring to the two lift augmentation curves of Figure 20, it is seen that there is an increase of augmentation of 1.4 at a value of  $h/D = .10$ . Since for the 1600-pound P-GEM an  $m_j v_j$  of 420 pounds would be required to hover at  $h/D = .10$ , the aerodynamic lift at this height at 35 miles per hour was computed to be  $1.4 \times 420$ , or 590 pounds. This reduced to a level attitude lift coefficient of 0.61 at this value of  $h/D$ .

Since higher forward speeds would produce higher aerodynamic lift, thereby increasing  $h/D$ , it was necessary to determine the variation in lift coefficient with  $h/D$  at zero angle of attack. This was done by referring to Figure 15, and these values were cross-plotted as shown in Figure 21. It will be noted that the flight-test-determined value of lift coefficient at  $h/D = .10$  of  $C'_L = .61$  falls on this curve constructed from wind-tunnel data. The maximum value of  $C_\mu$  obtainable in the wind tunnel was  $C_\mu = .04$ , while that value corresponding to 35 miles per hour for the full-scale craft was approximately twice the wind-tunnel momentum coefficient. That both the wind-tunnel and the full-scale P-GEM tests yielded the same value of lift coefficient with vastly different momentum coefficients was entirely coincidental and occurred because the wind tunnel lift included  $m_j v_j$  and the full scale results did not.

From the curve of Figure 21, values of  $C'_L$  were selected for several values of  $h/D$ . For these same values of  $h/D$ , lift augmentation ratio was determined from Figure 20 and aerodynamic lift was computed based upon the following expression:

$$L' = W - m_j v_j A.$$

Thus, given both the lift coefficient corresponding to a given value of  $h/D$  and the associated aerodynamic lift, the velocity was determined. The results of these several computations are shown in Figure 22, which relates the value of  $h/D$  with forward speeds of up to 65 miles per hour. By utilizing these techniques and information presented in Figures 18, 19, 20, 21 and 22, performance trade-offs can be made. An example of the type of trade-offs that can be made for a forward speed of 50 miles per hour follows.

1. At the same 1600-pound gross weight and at a velocity of 50 miles per hour,  $h/D$  is increased 100% over the hover value.
2. At no increase in  $h/D$  and at the same lift power, gross weight could be increased by 1000 pounds (a 60% increase).
3. At the same gross weight of 1600 pounds and allowing no change in  $h/D$  at 50 miles per hour, lift horsepower is reduced from

190 brake horsepower to 67 brake horsepower (a reduction of 65% in lift power required).

While these trade-off values are approximations based upon the extrapolated values of Figure 22, the flight test evidence is such as to lend strong support to these calculations.

---

### CONCLUSIONS

1. It can be concluded from this study that a GEM may indeed be so configured as to produce substantial gains in performance due to the aerodynamic lift of the craft at high speed.
2. The magnitude of the increase in performance is a function of the external shape of the craft, speed, and base loading.
3. A GEM can be simply stabilized and trimmed at speeds high enough to take advantage of aerodynamic lift.

## BIBLIOGRAPHY

1. Summers, Carr, Metzko, Nixon and Wojciechowiez, The General Characteristics of Winged Ground Effect Machines, TRECOM Technical Report 63-36, U. S. Army Transportation Research Command, Fort Eustis, Virginia, October 1963.
2. Kirschbaum, N., and Helgesen, J., Supplementary Lift for Air Cushion Vehicles, Volume II of III, TRECOM Technical Report 62-50, U. S. Army Transportation Research Command, Fort Eustis, Virginia, June 1962.
3. Helgesen, J., Some Effects of Forward Speed on the Performance of Air Cushion Vehicles, Memorandum RM-218, Grumman Aircraft Engineering Corporation, Bethpage, L. I., N. Y., November 1962.
4. Walker, N. K., Some Notes on the Lift and Drag of Ground Effect Machines, presented at LAS-NAVY National Meeting on Hydrofoils and Air Cushion Vehicles, Washington, D. C., September 19, 20, 1962.
5. Nixon, W. B., Sweeney, T. E., Preliminary Flight Experiments with the Princeton University Twenty-Foot Ground Effect Machine, Princeton Aero Report No. 506, January 1960.
6. Knowlton, M. P., Wojciechowiez, A. F., Jr., Model Studies of the Forward Flight Characteristics of the P-GEM, Princeton Aero Report No. 581, December 1961.

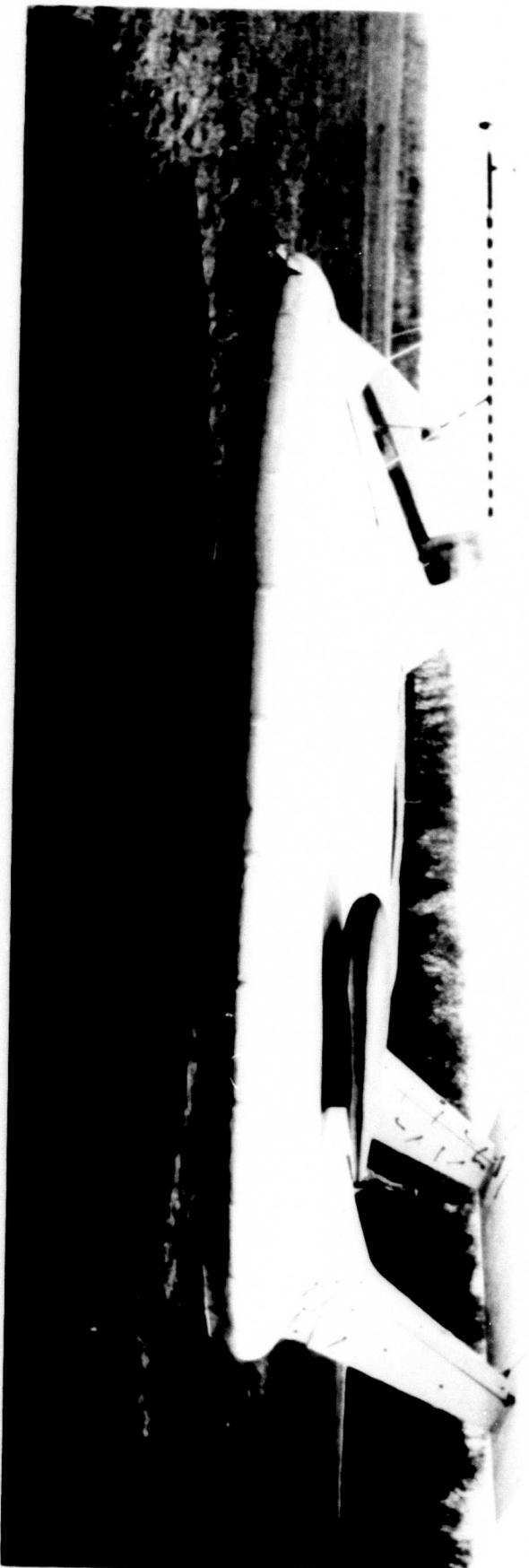


FIG. 1 P-GEM IN FORWARD FLIGHT

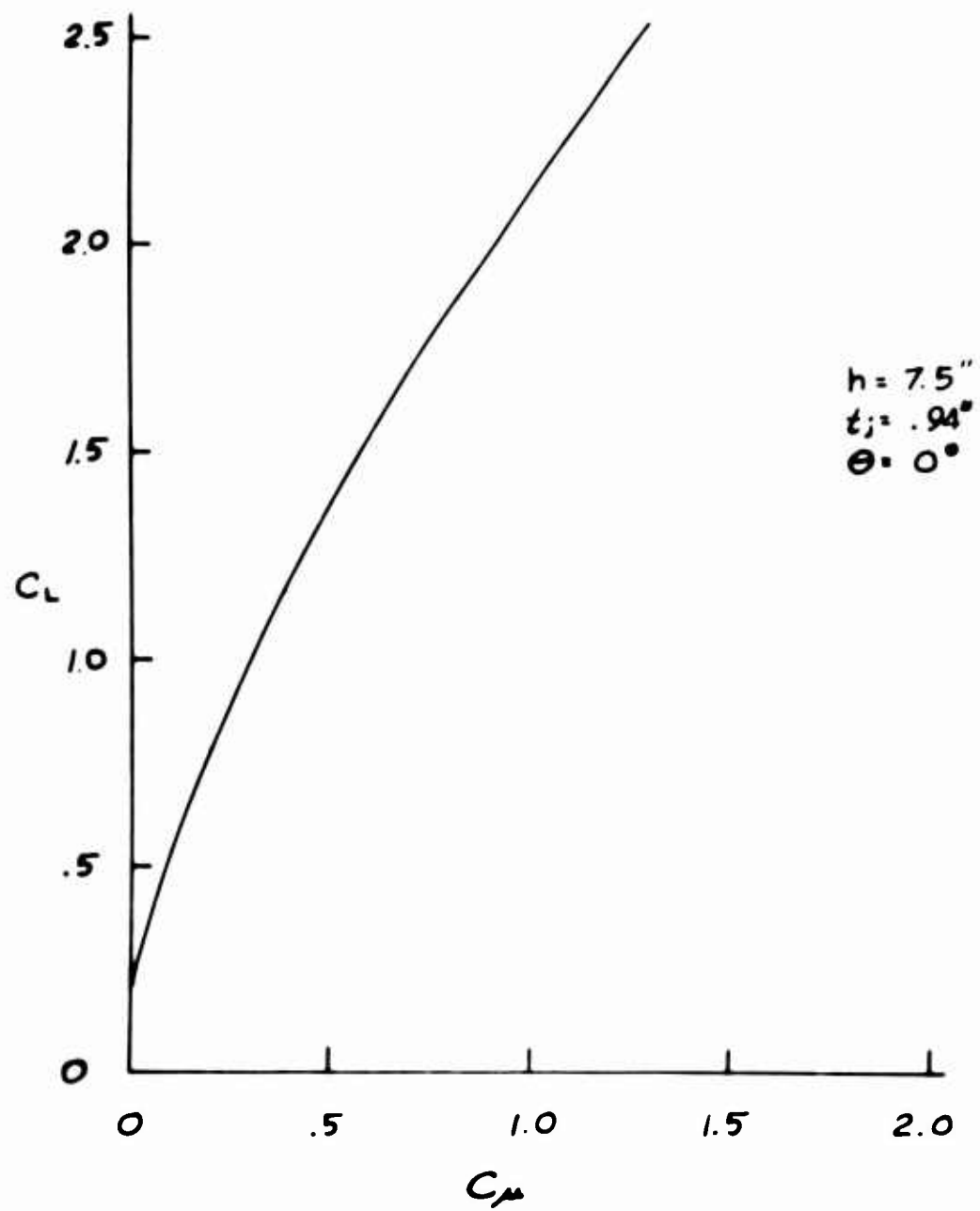


FIG. 2 LIFT COEFFICIENT VS. MOMENTUM COEFFICIENT

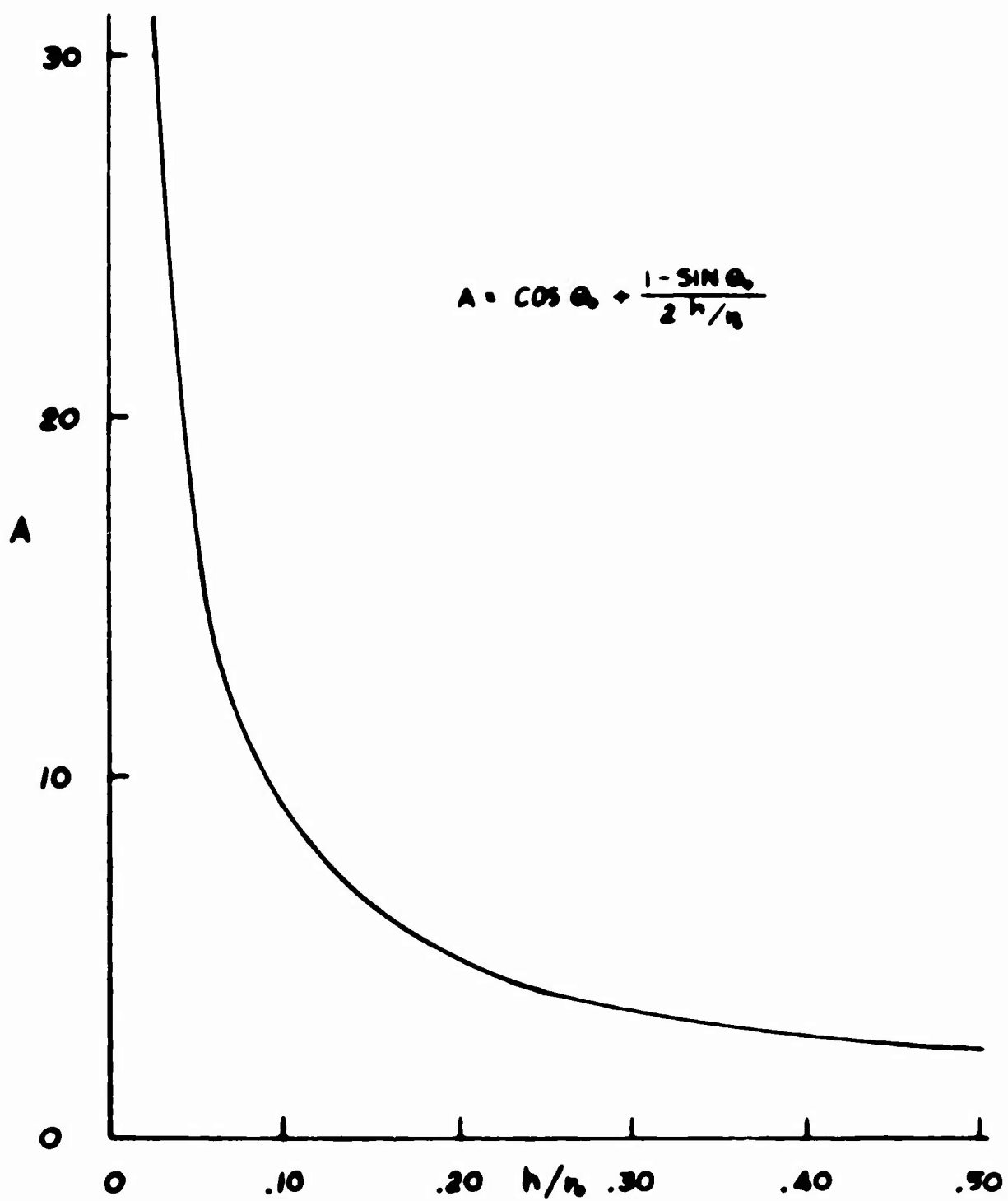


FIG. 3 THEORETICAL LIFT AUGMENTATION CURVE FOR A CIRCULAR GEM,  $\alpha_0 = 45^\circ$

Variable			E.
0.0	0.0	0.0	0.0
0.0	0.0	0.0	0.0
0.0	0.0	0.0	0.0

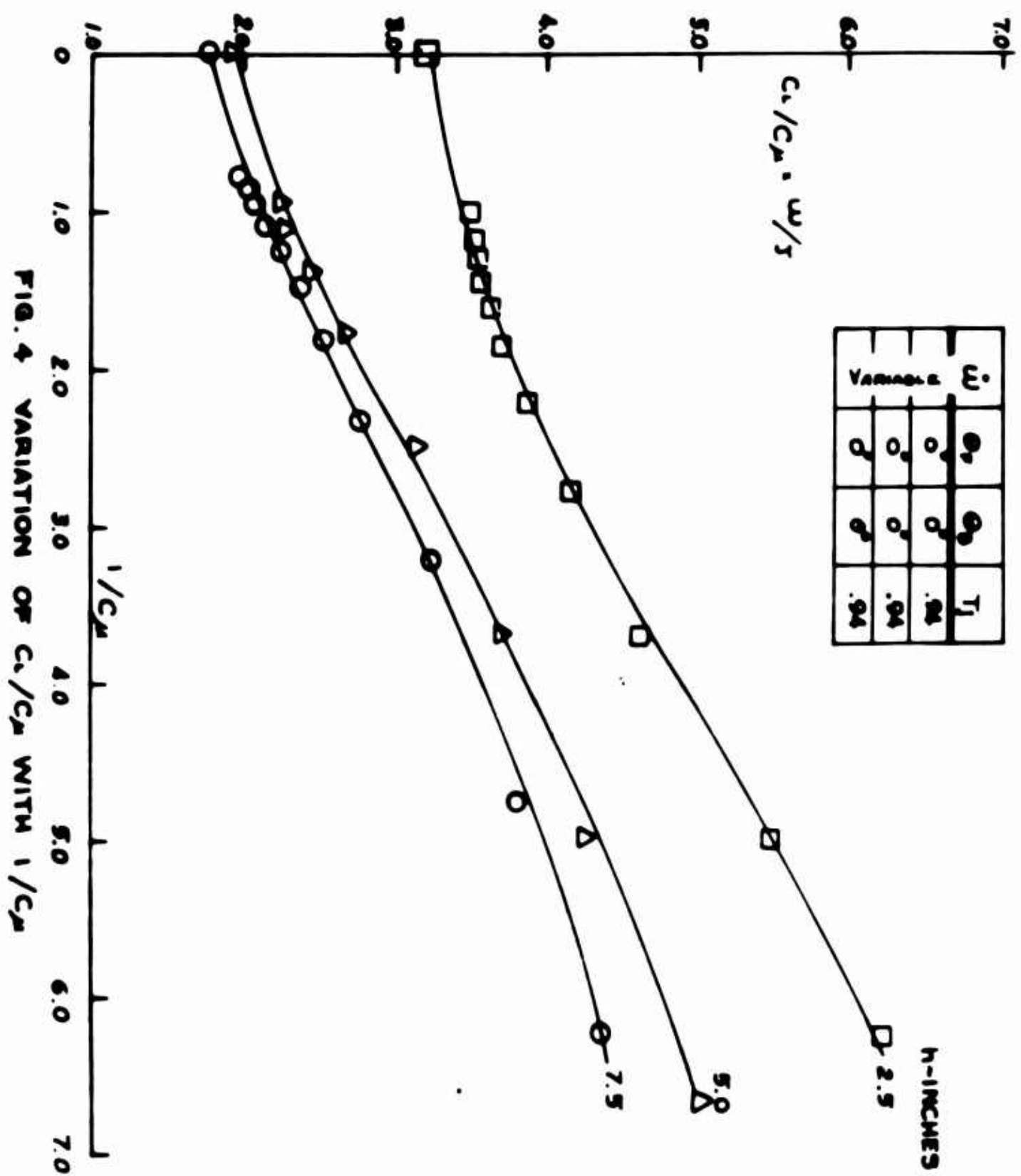


FIG. 4 VARIATION OF  $C_1/C_2$  WITH  $1/C_2$

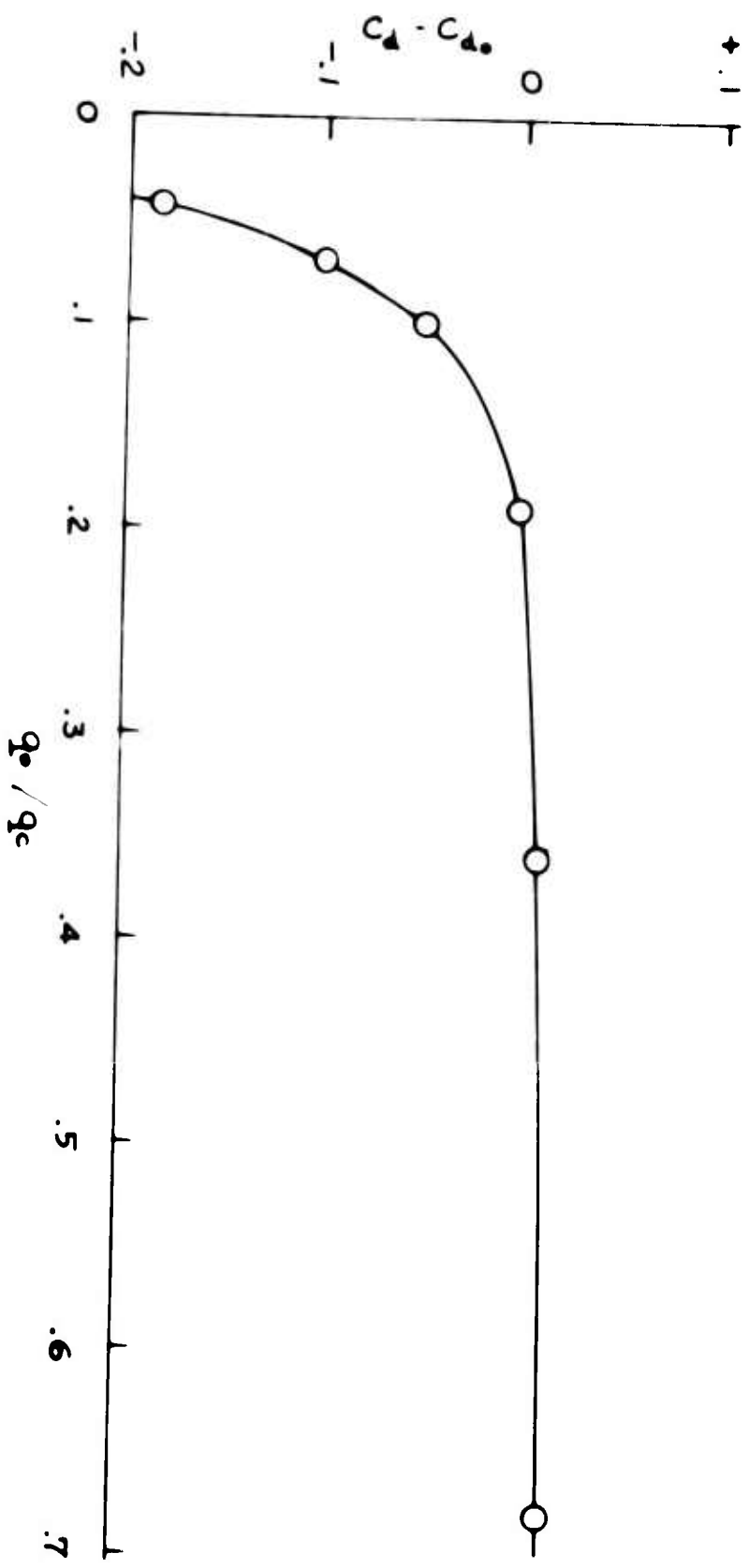


FIG. 5  $C_d - C_{d0}$  vs  $q_0 / q_c$

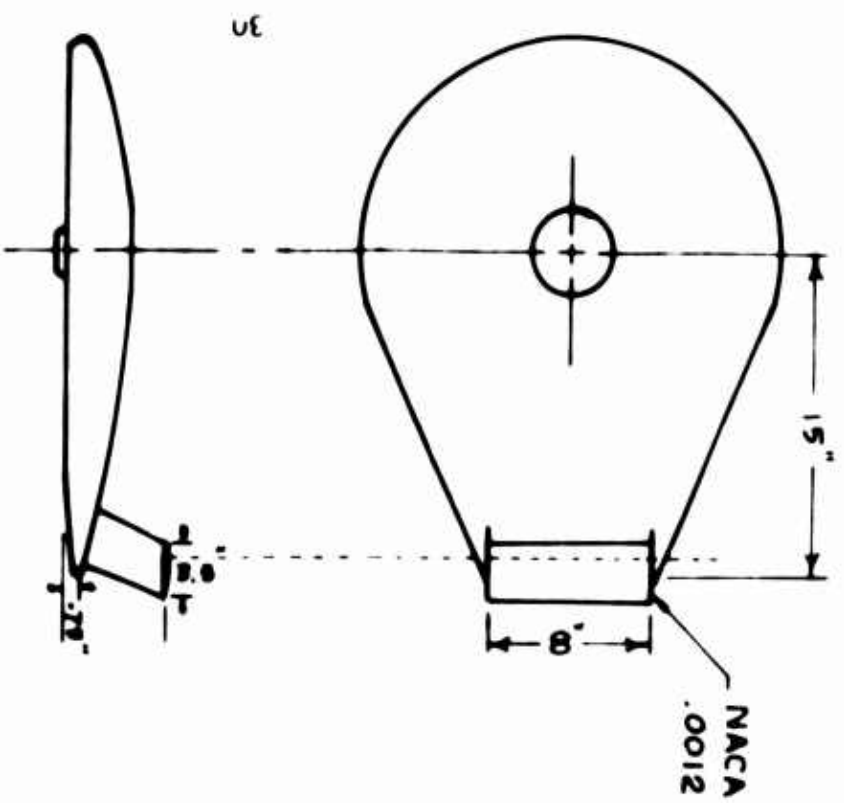


FIG. 6

BEAVER TAIL

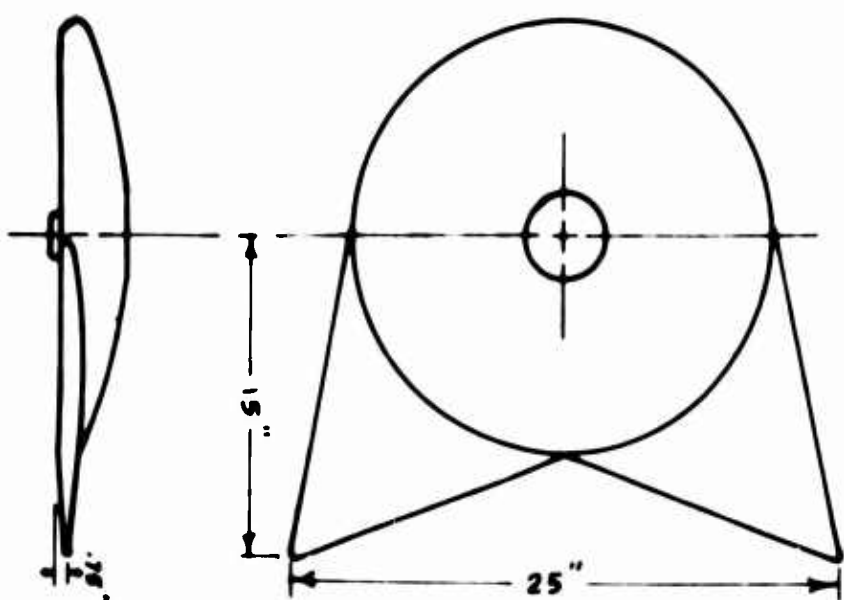


FIG. 7

SWEPT DELTA WING

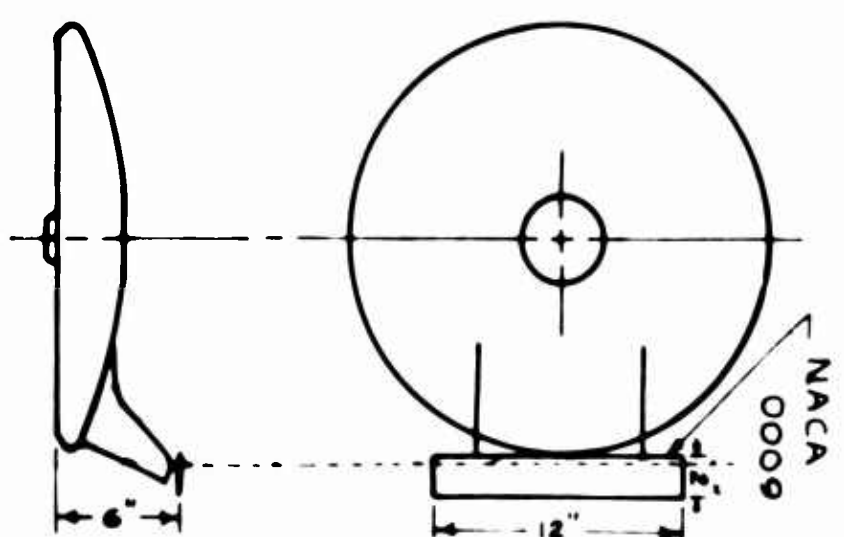


FIG. 8

GEARED TRIMMER

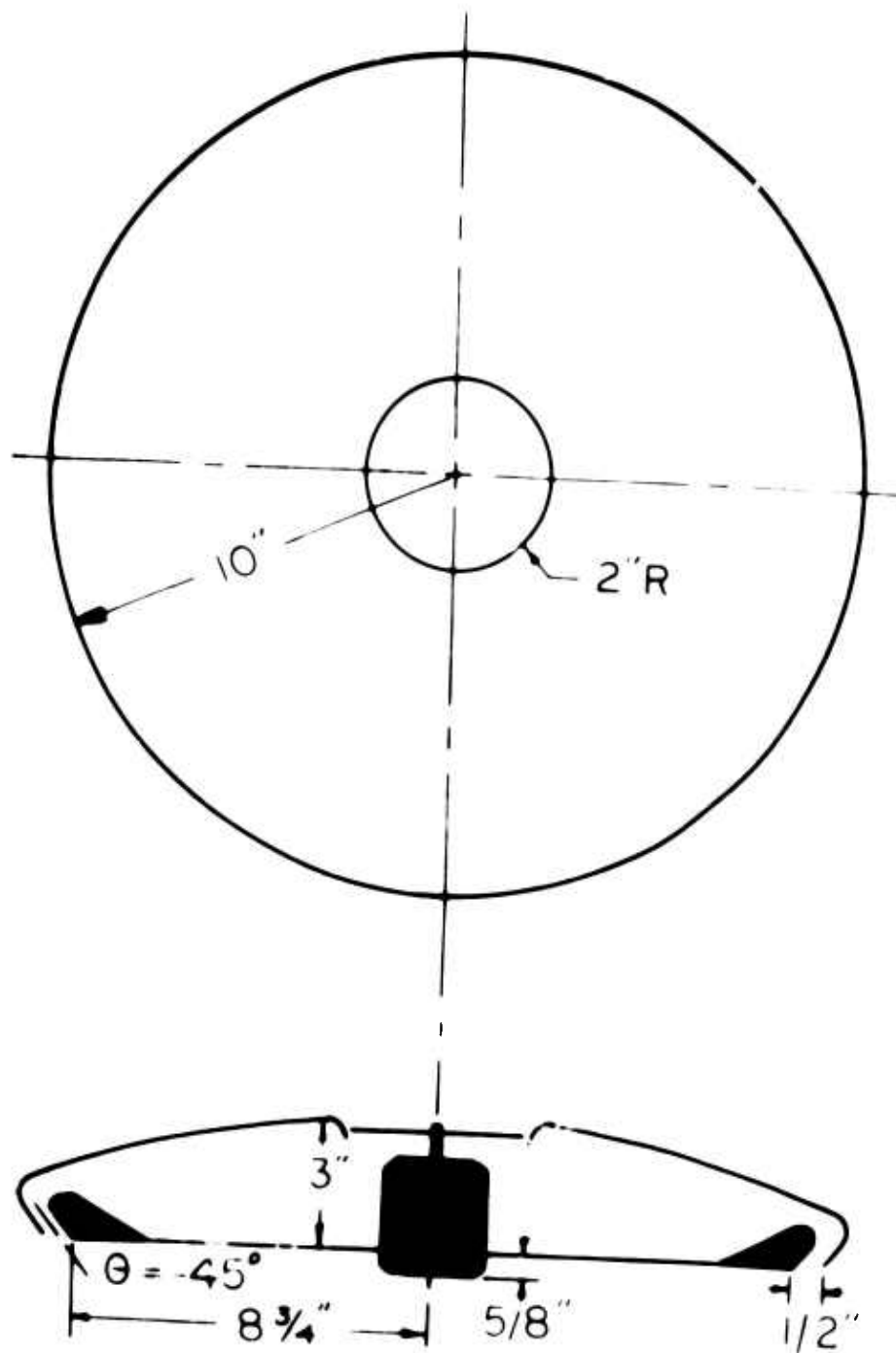


FIG. 9 SCHEMATIC LAYOUT AND BASIC DIMENSIONS  
OF 1/12 SCALE P-GEM MODEL

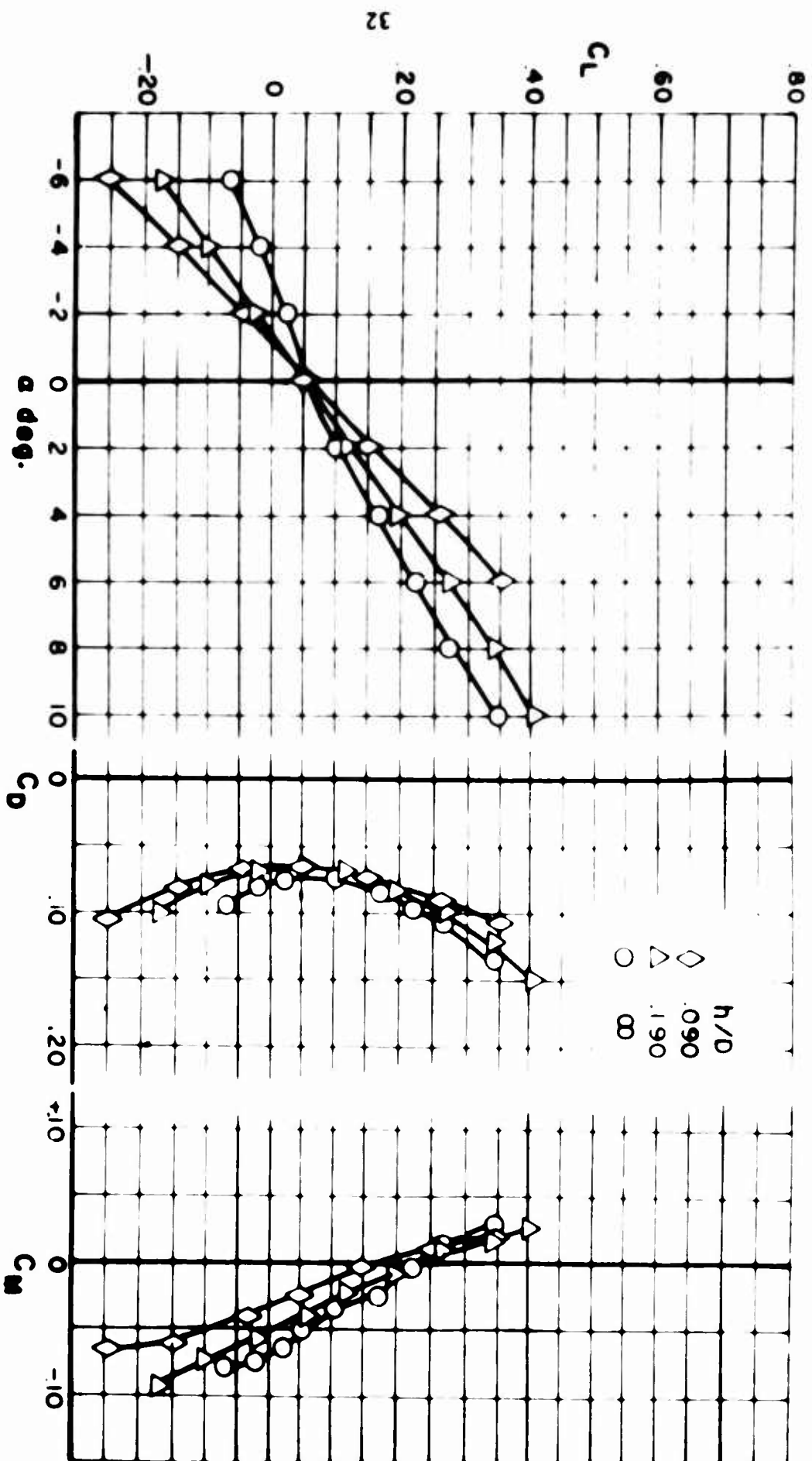


FIG. 10 CHARACTERISTICS OF THE BEAVER-TAILED P-GEM MODEL  
WITHOUT BLOWING

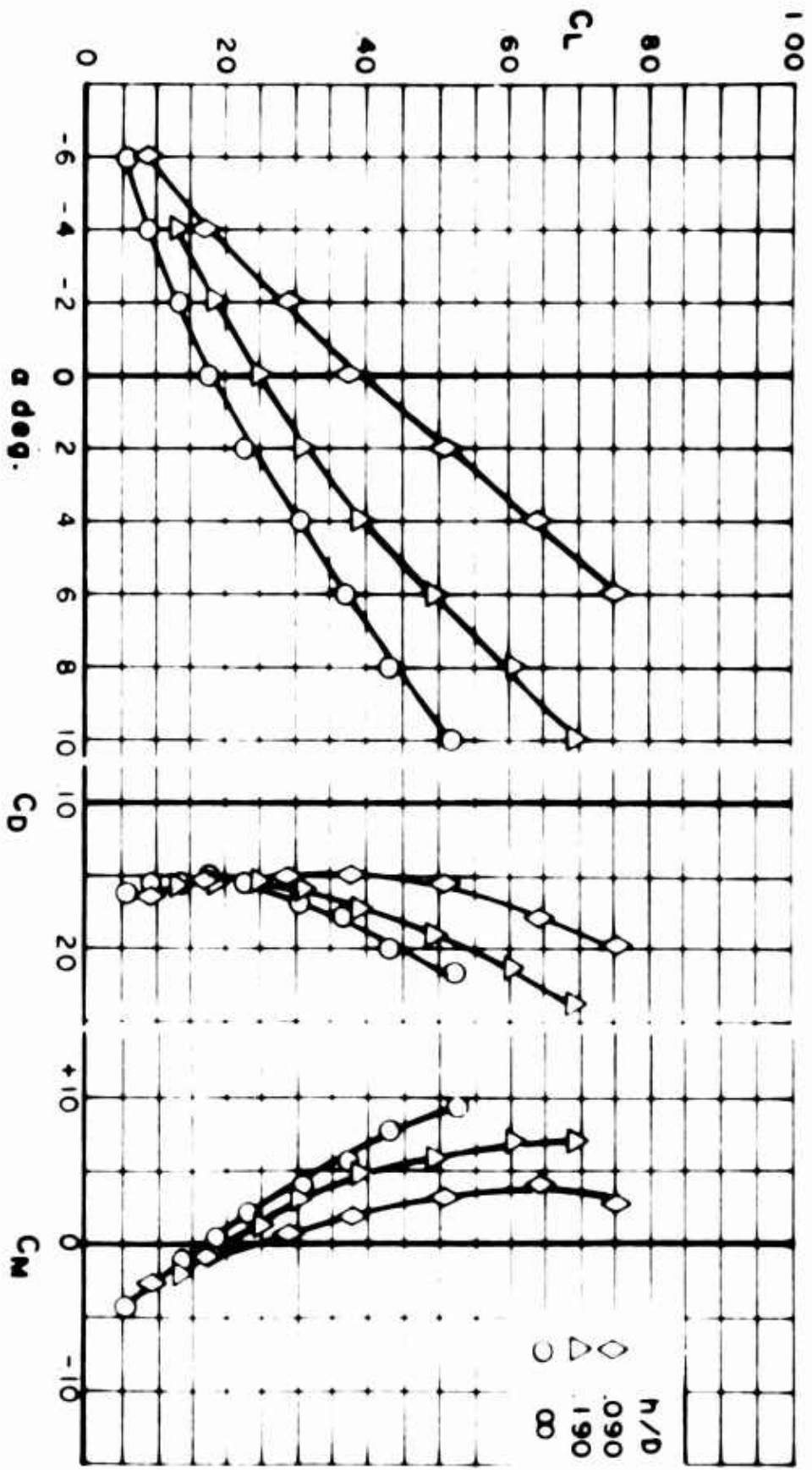


FIG. 11 CHARACTERISTICS OF THE BEAVER-TAILED P-GEM MODEL WITH BLOWING  $C_n = 0.04$

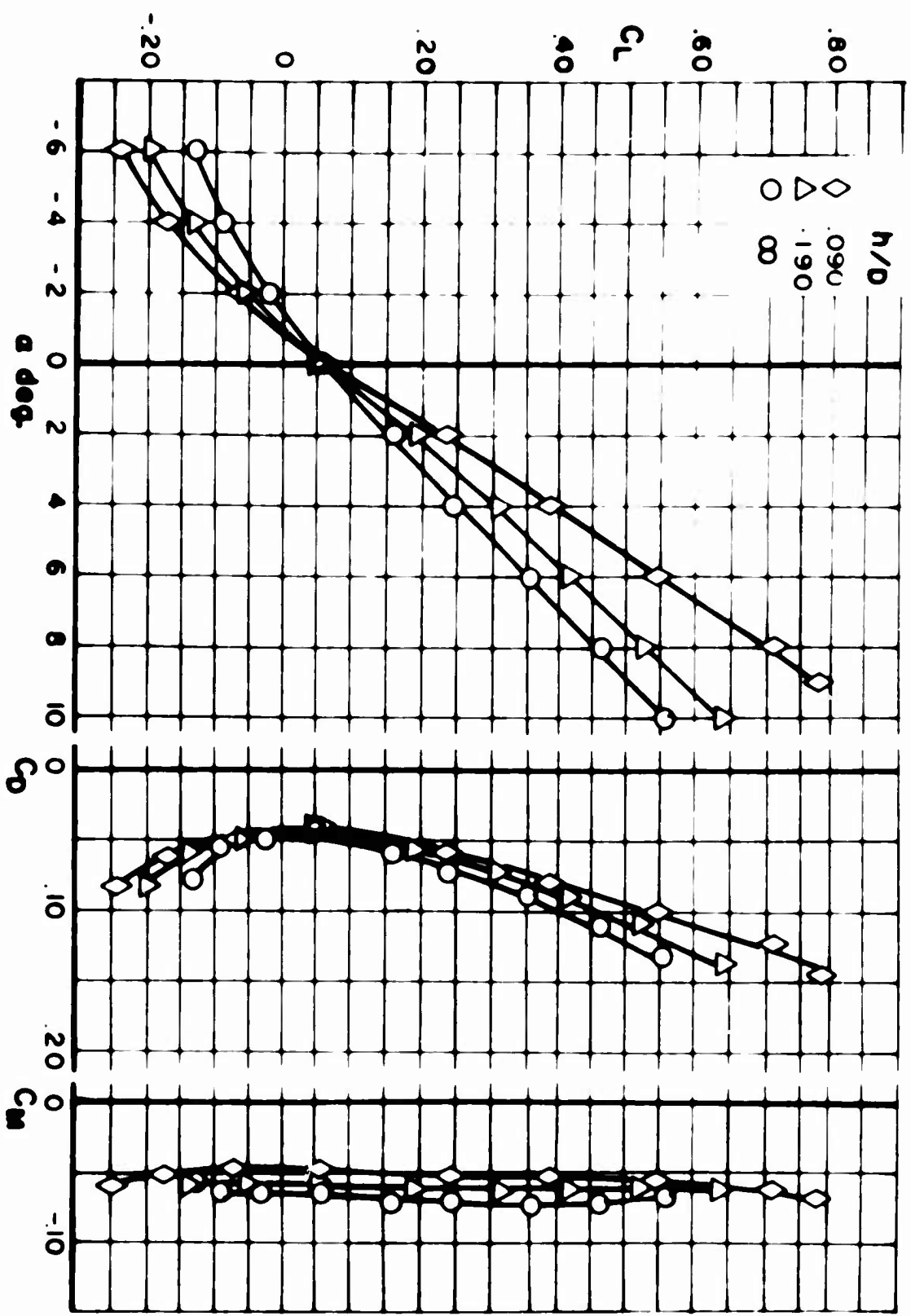


FIG. 12 CHARACTERISTICS OF THE DELTA-WINGED P-GEM MODEL  
WITHOUT BLOWING  $C_{\mu} = 0$

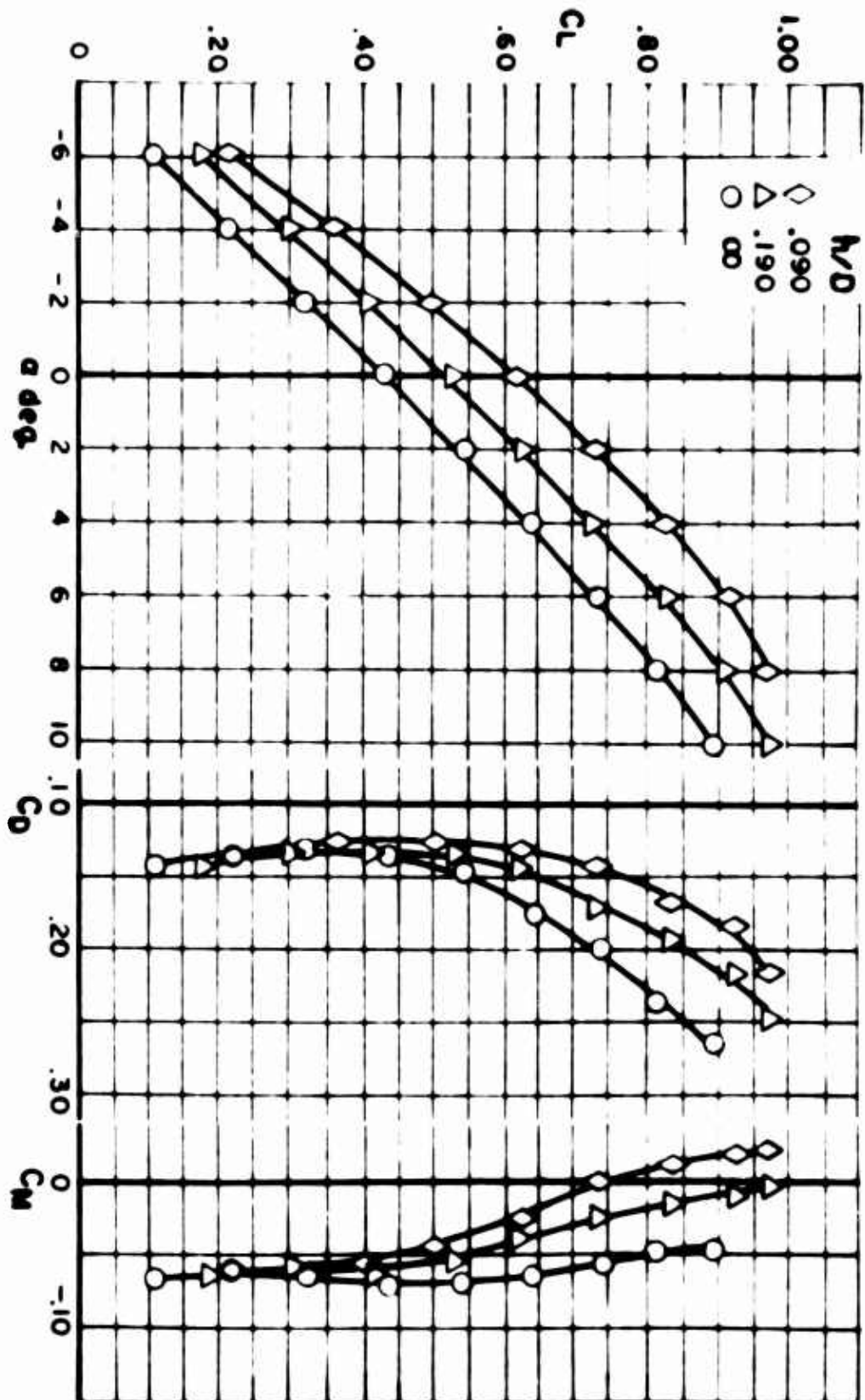


FIG. 13 CHARACTERISTICS OF THE DELTA-WINGED P-GEM MODEL  
WITH BLOWING  $C_u = .04$

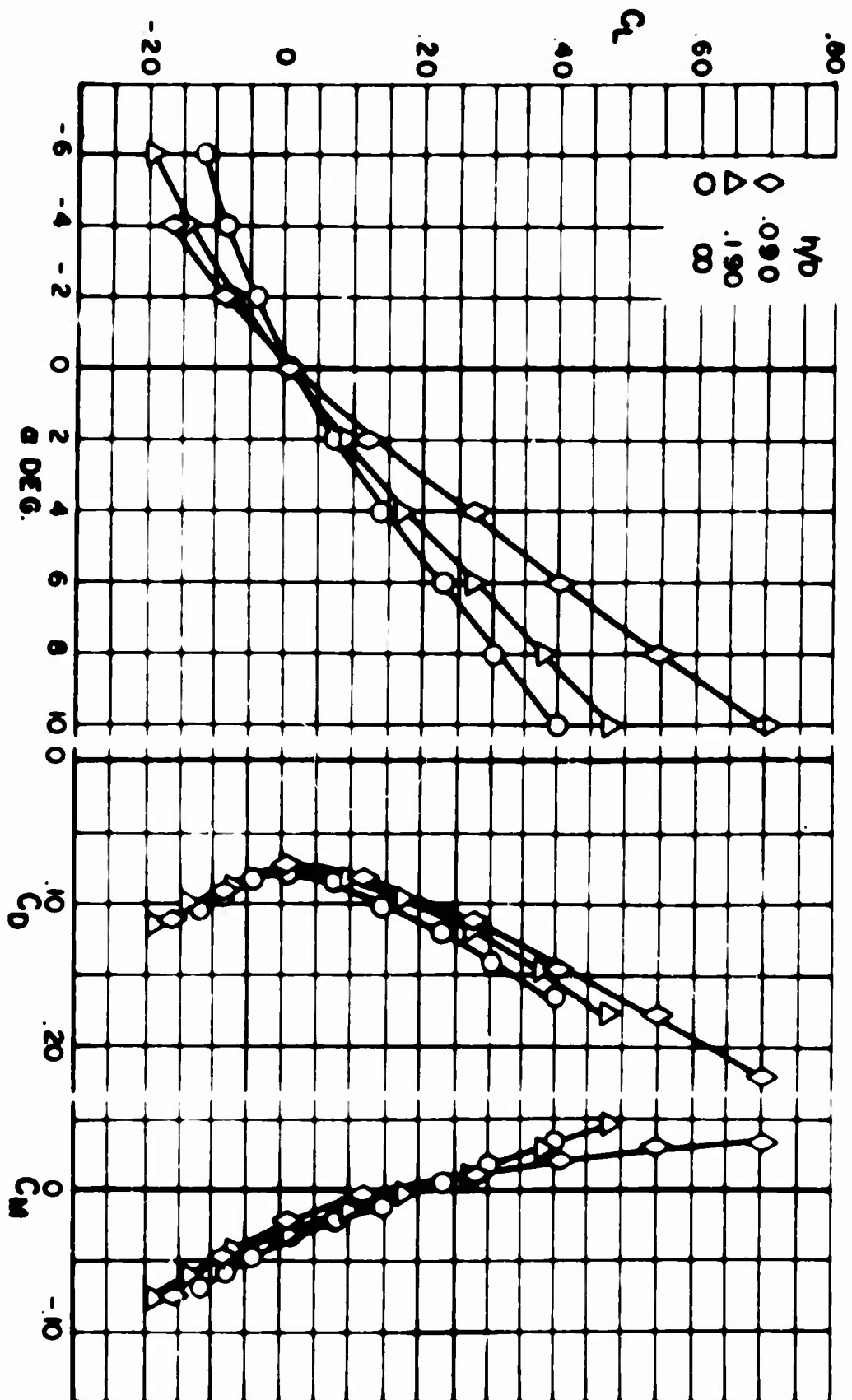


FIG. 14 CHARACTERISTICS OF THE TRIMMER TAILED P-GEM MODEL  
WITHOUT BLOWING  $C_M = 0$

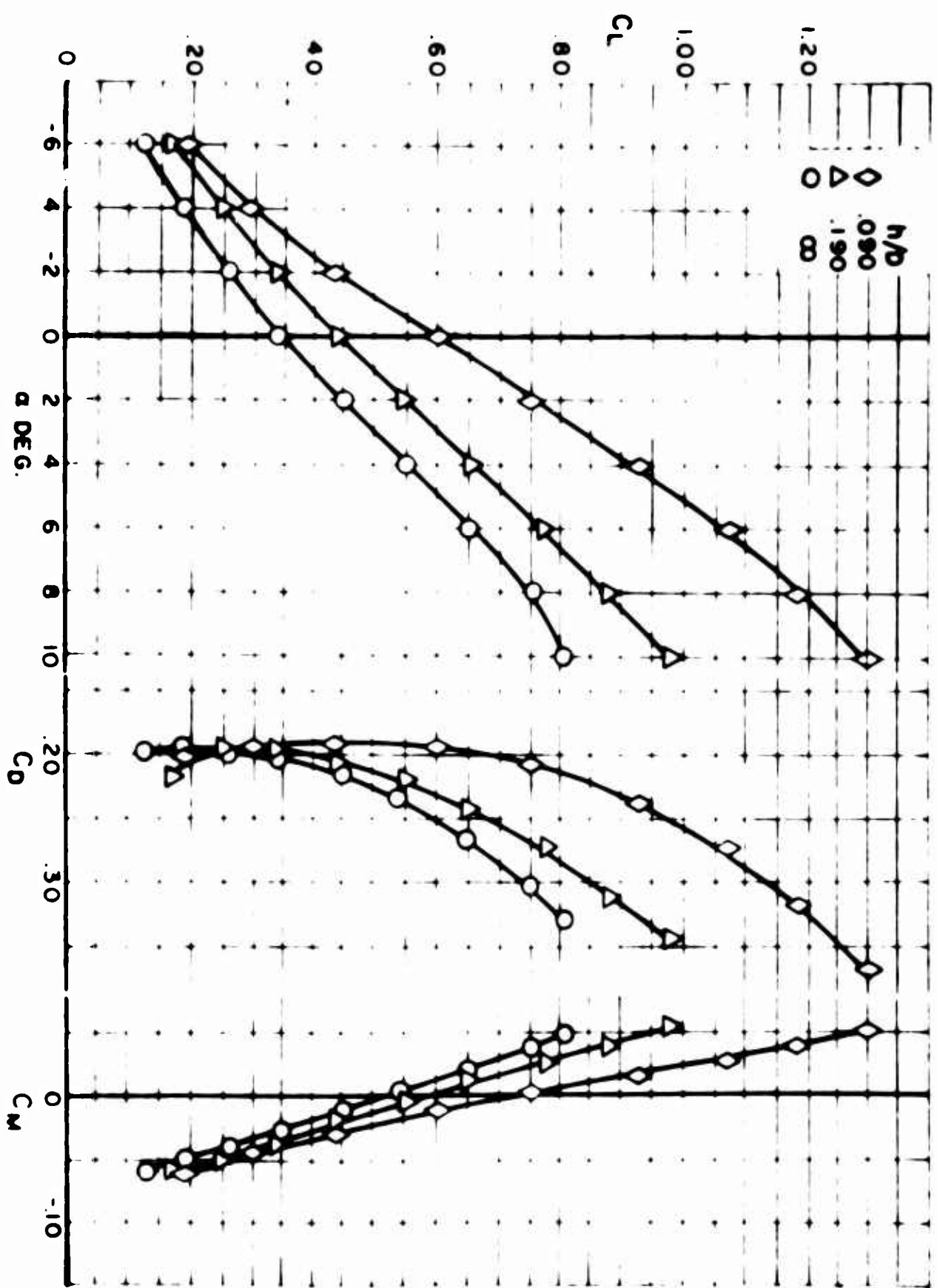


FIG. 15 CHARACTERISTICS OF THE TRIMMER TAILED P-GEM MODEL  
WITH BLOWING  $C_{\mu} = .04$

FIG. 16 CHARACTERISTICS OF THE P-GEH MODEL WITH TRIMMER TAIL AND  
BLOWING  $h/d = 0.030$   $C_{\mu} = .04$

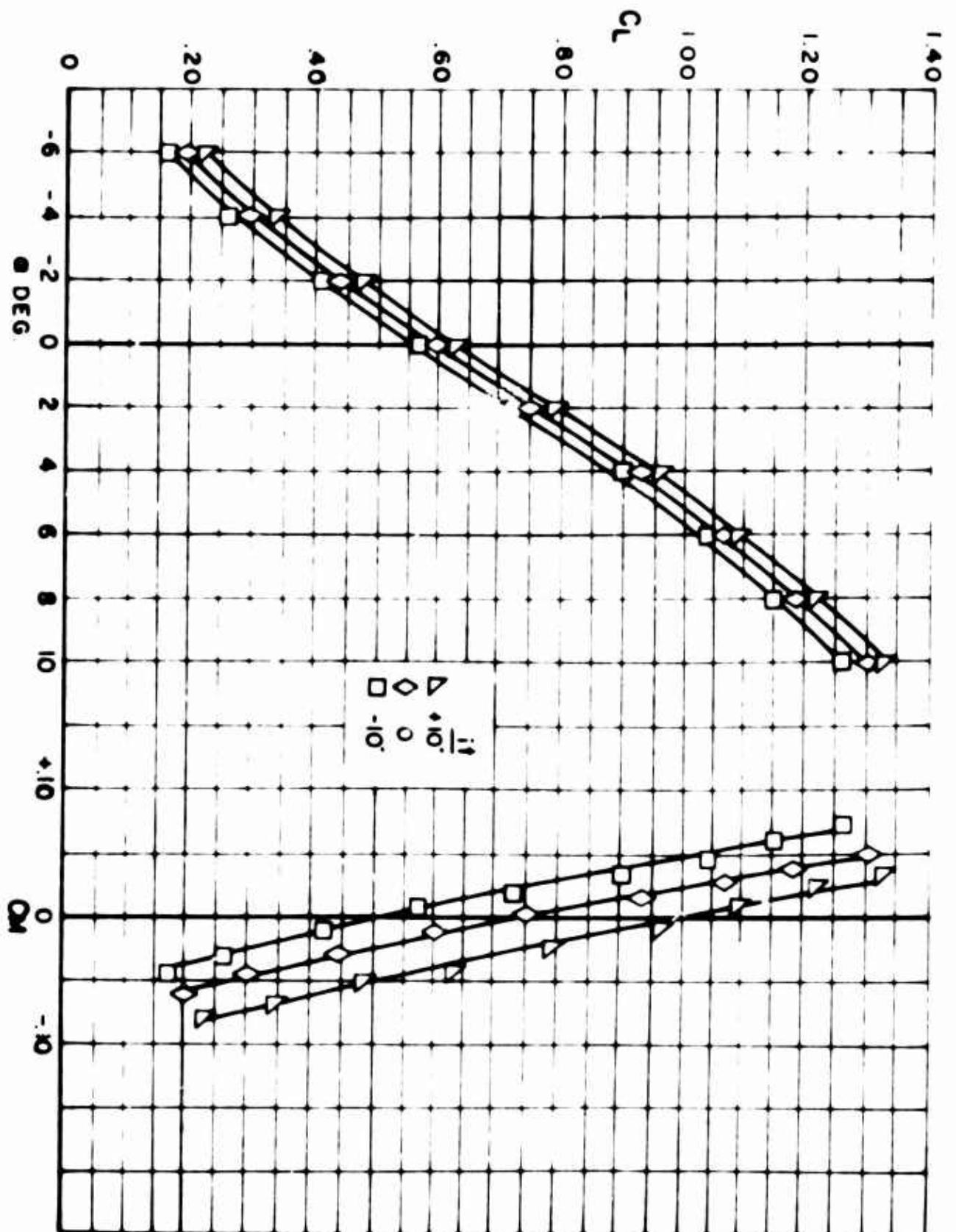




FIG. 17 HEIGHT SENSOR INSTALLED ON P-GEM

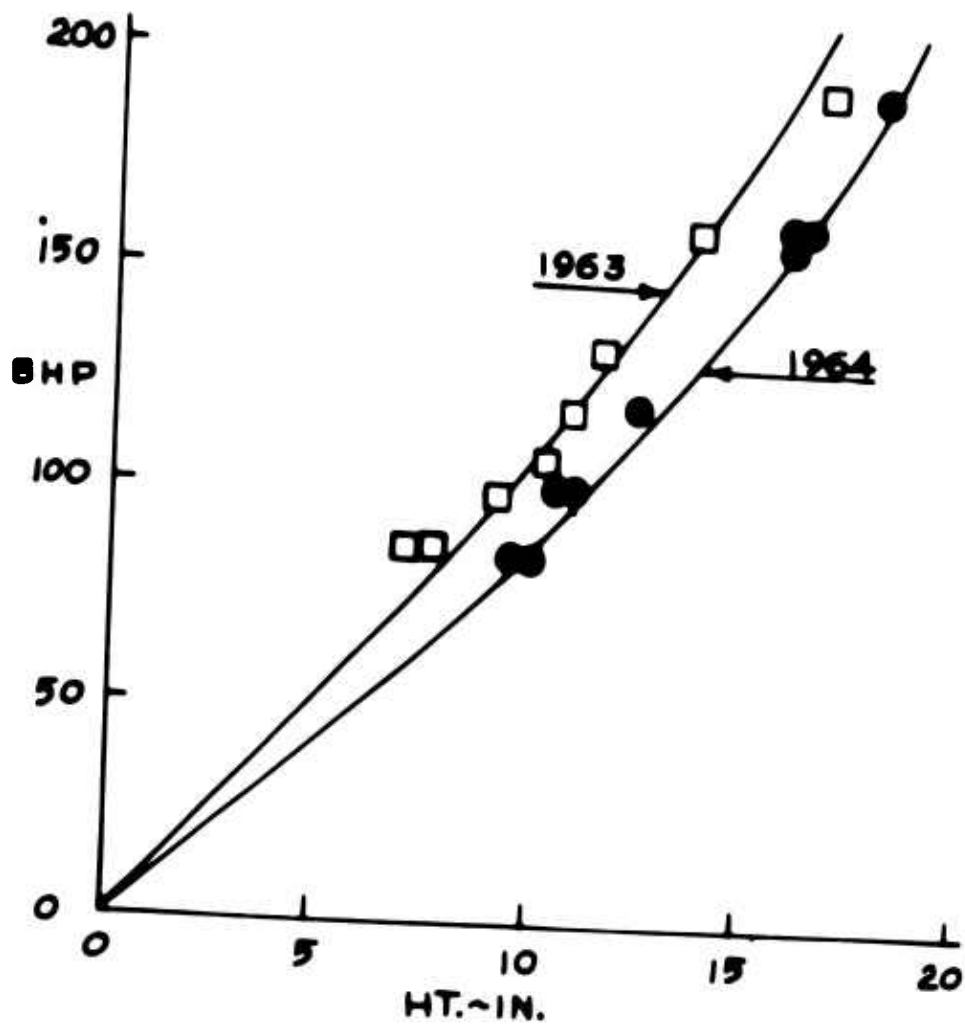


FIG. 18 HOVER HEIGHT VS. BRAKE HORSEPOWER,  
P-GEM

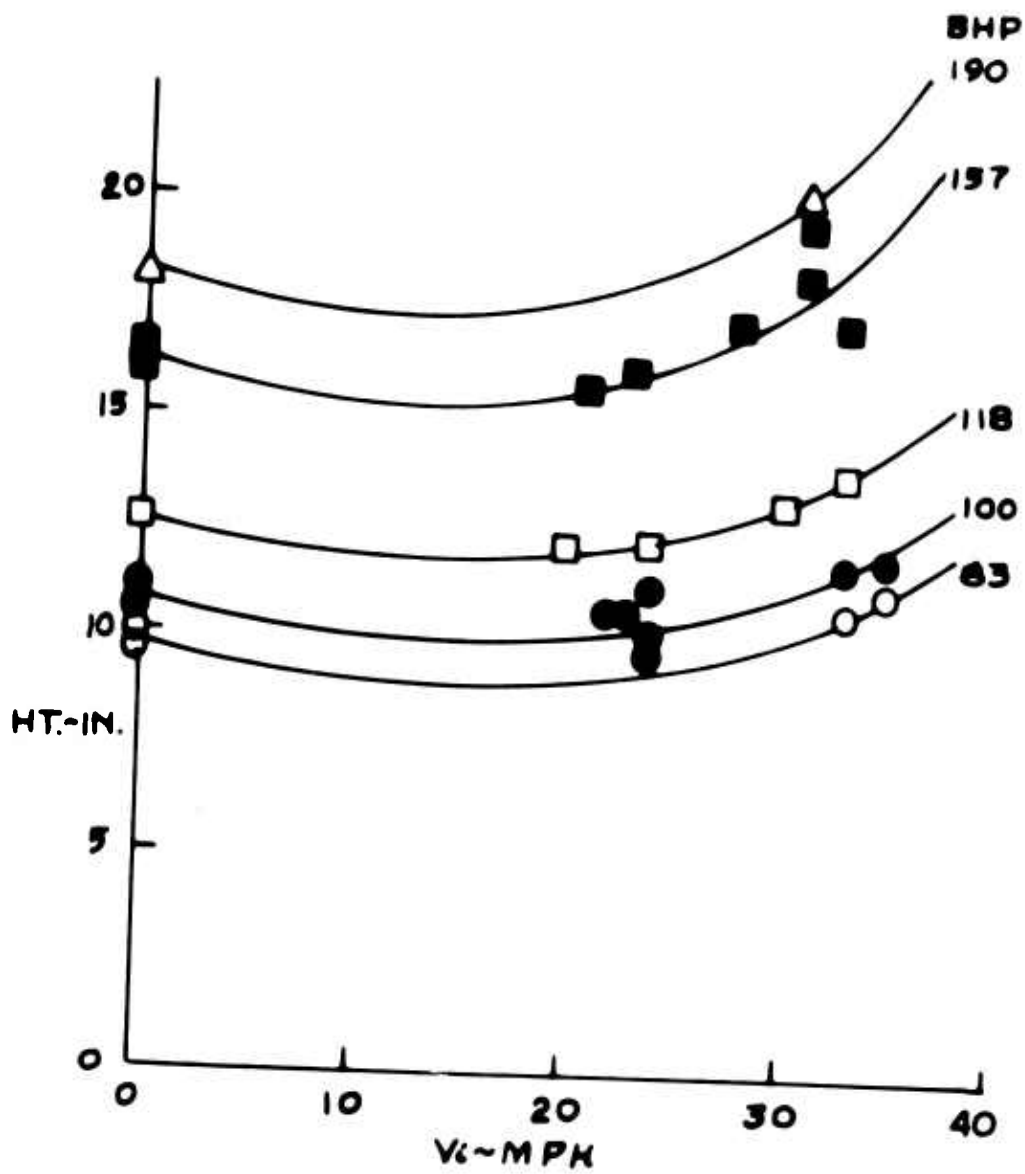


FIG. 19 HEIGHT VS. VELOCITY VS. LIFT POWER , P-GEM

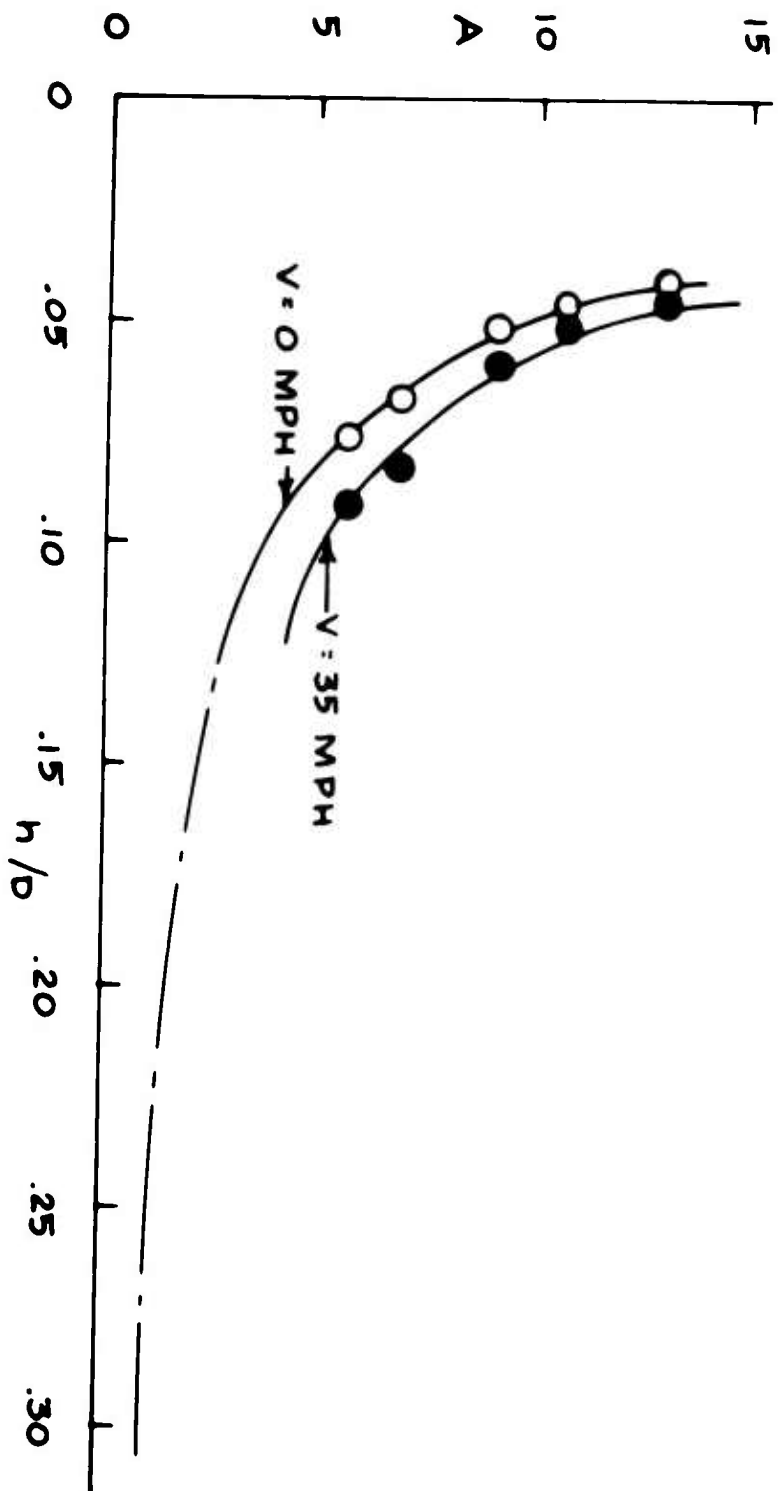


FIG. 20 LIFT AUGMENTATION RATIO VS.  $h/D$  VS. AIRSPEED, P-GEM

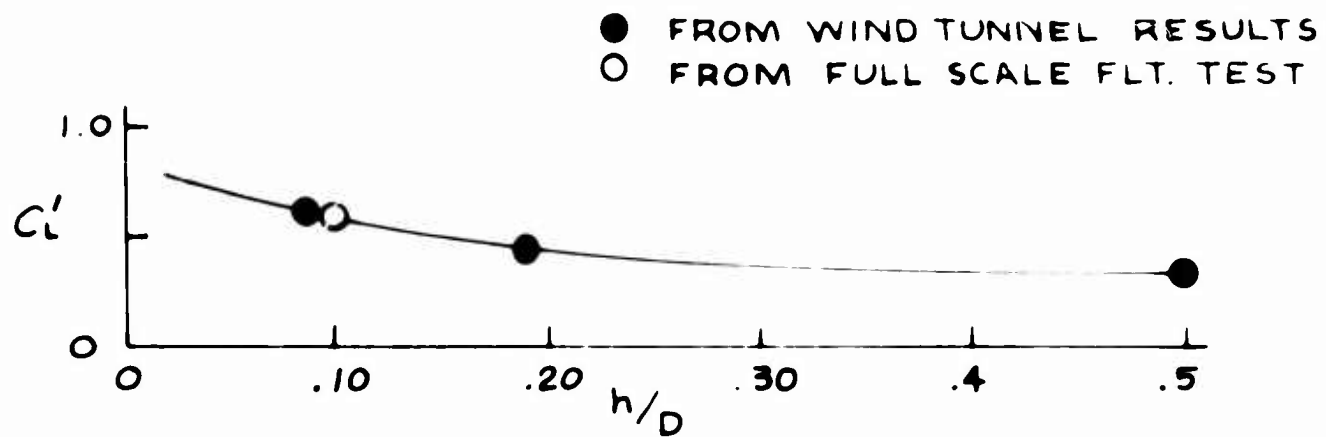


FIG. 21 VARIATION OF  $C_L'$  WITH  $h/D$

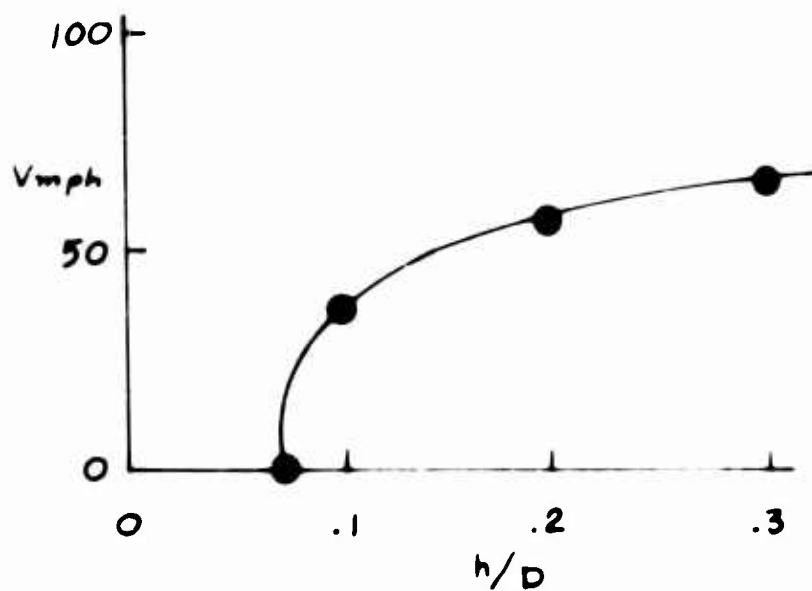


FIG. 22 EXTRAPOLATED  $h/D$  VS VELOCITY, P-GEM

## DISTRIBUTION

U. S. Army Materiel Command	
U. S. Army Mobility Command	
U. S. Army Aviation Materiel Command	
U. S. Strike Command	
Chief of R&D, D/A	
U. S. Army Transportation Research Command	6
U. S. Army Research and Development Group (Europe)	
U. S. Army Engineer Research and Development Laboratories	
U. S. Army Human Engineering Laboratories	
Army Research Office-Durham	
U. S. Army Research Support Group	
U. S. Army Medical Research and Development Command	
U. S. Army Engineer Waterways Experiment Station	
U. S. Army Combat Developments Command	
Transportation Agency	
U. S. Army War College	
U. S. Army Command and General Staff College	1
U. S. Army Transportation School	1
U. S. Army Tank-Automotive Center	2
U. S. Army General Equipment Test Activity	1
U. S. Army Arctic Test Center	1
U. S. Army Airborne, Electronics and Special Warfare Board	1
Chief of Naval Operations	1
Bureau of Ships	1
Bureau of Naval Weapons	2
Bureau of Supplies and Accounts, N/D	1
U. S. Naval Supply Research and Development Facility	1
U. S. Naval Postgraduate School	1
David Taylor Model Basin	1
Marine Corps Landing Force Development Center	1
Marine Corps Educational Center	1
Marine Corps Liaison Officer, U. S. Army Transportation School	1
Ames Research Center, NASA	2
NASA-LRC, Langley Station	2
Lewis Research Center, NASA	2
NASA Representative, Scientific and Technical Information Facility	2



Princeton University, Department of Aerospace & Mechanical Sciences, Princeton, New Jersey, THE DOMINANT AERODYNAMIC CHARACTERISTICS OF A SHAPED GEM - A. F. Wojciechowicz, Jr., W. B. Nixon, and T. E. Sweeney, September 1964, Report No. 684, 45 pp. (Contract DA 44-177-TC-850) USATRECOM Task 1D02170A04803 Report 64-45.

Unclassified Report

The effect of aerodynamic forces and moments acting on a ground effect machine in forward flight are theoretically and experimentally investigated. The study emphasized the stability and performance of such craft.

Princeton University, Department of Aerospace & Mechanical Sciences, Princeton, New Jersey, THE DOMINANT AERODYNAMIC CHARACTERISTICS OF A SHAPED GEM - A. F. Wojciechowicz, Jr., W. B. Nixon, and T. E. Sweeney, September 1964, Report No. 684, 45 pp. (Contract DA 44-177-TC-850) USATRECOM Task 1D02170A04803 Report 64-45.

Unclassified Report

The effect of aerodynamic forces and moments acting on a ground effect machine in forward flight are theoretically and experimentally investigated. The study emphasized the stability and performance of such craft.

1. Ground Effect Machine
2. Contract DA 44-177-TC-850

Princeton University, Department of Aerospace & Mechanical Sciences, Princeton, New Jersey, THE DOMINANT AERODYNAMIC CHARACTERISTICS OF A SHAPED GEM - A. F. Wojciechowicz, Jr., W. B. Nixon, and T. E. Sweeney, September 1964, Report No. 684, 45 pp. (Contract DA 44-177-TC-850) USATRECOM Task 1D02170A04803 Report 64-45.

Unclassified Report

The effect of aerodynamic forces and moments acting on a ground effect machine in forward flight are theoretically and experimentally investigated. The study emphasized the stability and performance of such craft.

1. Ground Effect Machine
2. Contract DA 44-177-TC-850

Princeton University, Department of Aerospace & Mechanical Sciences, Princeton, New Jersey, THE DOMINANT AERODYNAMIC CHARACTERISTICS OF A SHAPED GEM - A. F. Wojciechowicz, Jr., W. B. Nixon, and T. E. Sweeney, September 1964, Report No. 684, 45 pp. (Contract DA 44-177-TC-850) USATRECOM Task 1D02170A04803 Report 64-45.

Unclassified Report

The effect of aerodynamic forces and moments acting on a ground effect machine in forward flight are theoretically and experimentally investigated. The study emphasized the stability and performance of such craft.

1. Ground Effect Machine
2. Contract DA 44-177-TC-850

1. Ground Effect Machine
2. Contract DA 44-177-TC-850